

It's About Time: Temporal References in Emergent Communication

Olaf Lipinski¹

Adam J. Sobey^{1,2}

Federico Cerutti³

Timothy J. Norman¹

O.LIPINSKI@SOTON.AC.UK

AJS502@SOTON.AC.UK

FEDERICO.CERUTTI@UNIBS.IT

T.J.NORMAN@SOTON.AC.UK

¹University of Southampton, ²The Alan Turing Institute, ³University of Brescia

Editor: N/A

Abstract

Emergent communication studies the development of language between autonomous agents, aiming to improve understanding of natural language evolution and increase communication efficiency. While temporal aspects of language have been considered in computational linguistics, there has been no research on temporal references in emergent communication. This paper addresses this gap, by exploring how agents communicate about temporal relationships. We analyse three potential influences for the emergence of temporal references: environmental, external, and architectural changes. Our experiments demonstrate that altering the loss function is insufficient for temporal references to emerge; rather, architectural changes are necessary. However, a minimal change in agent architecture, using a different batching method, allows the emergence of temporal references. This modified design is compared with the standard architecture in a temporal referential games environment, which emphasises temporal relationships. The analysis indicates that over 95% of the agents with the modified batching method develop temporal references, without changes to their loss function. We consider temporal referencing necessary for future improvements to the agents' communication efficiency, yielding a closer to optimal coding as compared to purely compositional languages. Our readily transferable architectural insights provide the basis for their incorporation into other emergent communication settings.

Keywords: Emergent Communication, Emergent Language, Temporal Logic, Multiagent Systems, Representation Learning

1 Introduction

In Emergent Communication (EC), autonomous agents develop their language from scratch. This results in a vocabulary that is tailored to the specific environment in which they have been trained, reflecting the tasks the agents perform, the actions available to them and the other agents they interact with. These properties make the emergent language memory and bandwidth efficient, as the agents can optimise their vocabulary size and word length to their specific task, providing an advantage over a general communication protocol (Rita et al., 2020).

Many aspects of emergent language have been explored (Lazaridou and Baroni, 2020; Boldt and Mortensen, 2024), with a particular focus on improving communication efficiency

(Rita et al., 2020; Chaabouni et al., 2019; Kang et al., 2020). Kang et al. (2020) demonstrate how using the minimal deviation between subsequent time steps allows for more concise communication by reducing redundant information transfer. Investigation of the contextual information of the resulting language offered a further improvement in agent performance by using the time step similarity together with optimisation of the reconstruction of the speaker’s state (Kang et al., 2020). There is, however, no existing research investigating or reporting on the emergence of temporal referencing strategies, where agents could communicate about relationships between different time steps.

Such temporal references, together with the general characteristics of emergent languages, will enhance the agent’s bandwidth efficiency and task performance in a variety of situations. As environmental complexity is being scaled in emergent communication research (Chaabouni et al., 2022), temporal references will benefit agents in settings where temporal relationships are embedded. One example is social deduction games (Brandizzi et al., 2021; Lipinski et al., 2022; Koppurapu et al., 2022), where referencing past events are expected to be key to winning strategies. Temporal references will allow agents to develop more efficient methods of communication by assigning shorter messages to events that happen more often. This is similar to Zipf’s Law in human languages (Zipf, 1949), which states that the most commonly used words are the shortest.

Temporal references would be particularly effective when the distribution of observations would be non-uniform, which means that certain objects appear more often than others. Specialised messages, used only for temporal references, would then also become more frequent than others. From information theory, we know that (adaptive) Huffman coding (Huffman, 1952; Knuth, 1985; Vitter, 1987) can assign shorter bit sequences to more frequent messages, thereby compressing them more efficiently than less common messages. Consequently, the incorporation of temporal references can enhance the efficiency of transmitting emergent language, optimizing communication.

Our contribution lies in examining when temporal references emerge between agents. Three potential prerequisites are explored: environmental pressures, external pressures and architectural changes. The agents are trained in both the regular referential game (Lazaridou et al., 2017) and on an environment which encourages the development of temporal references through embedded environmental pressures (Section 2.3). The effect of an external pressure to develop temporal referencing is explored via an additional loss applied to the agents (Section 5). Three types of architecture are evaluated, (Section 3), analysing two novel architectures together with a reference architecture based on the commonly used EGG (Kharitonov et al., 2019) agents. The baseline *Base* (Section 3.1) agent, provides us with a reference performance for both the emergence of temporal references, and performance in an environment. This baseline is compared to a *Temporal* (Section 3.2) agent, which features a sequentially batched LSTM, instead of the parallel batching used in EGG, which allows the agents to build an understanding of the target sequence. Additionally, the *TemporalR* (Section 3.3) agent combines the information from the sequential LSTM and the parallel batched LSTM from the *Base* agent. This allows it to process information about the objects, without needing to focus on their order in the sequence at the same time.

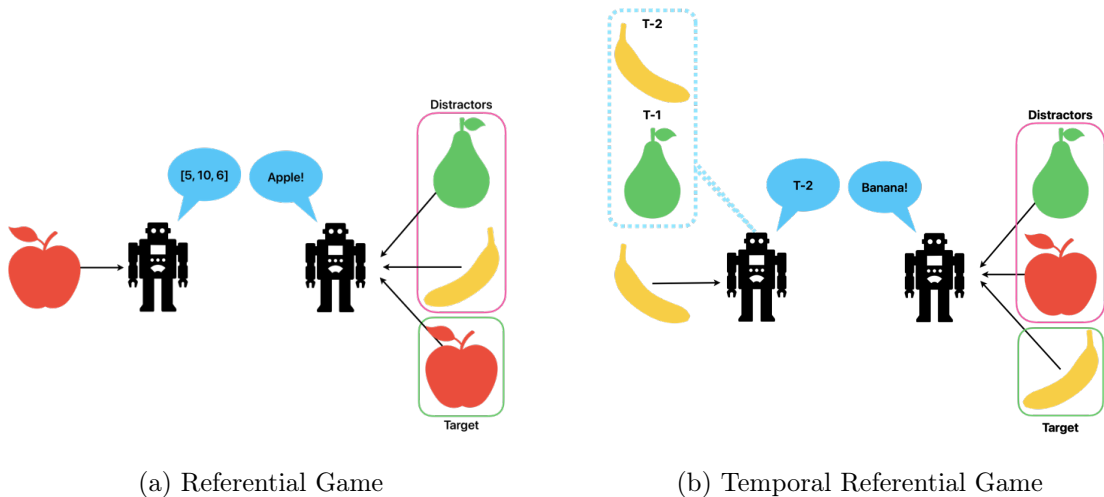


Figure 1: Structure of the referential game and temporal referential game.

2 Temporal Referential Games

Our experiments are based on classic referential games (Lewis, 1969; Lazaridou et al., 2018). The most commonly used framework to study emergent communication, EGG (Kharitonov et al., 2019), as well as other works (Chaabouni et al., 2020; Taillandier et al., 2023; Bosc, 2022; Ueda and Washio, 2021), uses two agents: a sender and a receiver. The sender begins the game by observing a target object, which could be represented by an image or a vector, and then generates a message. This message is passed to the receiver, along with the target object and a number of distractor objects. The receiver’s task is to discern the target object from among the objects it observes, using the information contained in the message it receives. This exchange is repeated every episode. The referential game is presented in Figure 1a.

Referential games with attribute-value vectors are used to isolate and limit the external factors that could impact the performance of the agents. An image-based representation of the objects is used to separate the performance of the agent from the training and performance of a vision network, and to reduce the computational requirements of our experiments. Additionally, the output of a vision layer can be considered as a representation of the object attributes, which could be approximated by the vectors used in our setup instead.

This common approach from EC (Kharitonov et al., 2019; Chaabouni et al., 2020; Ueda et al., 2022), is a well-known test bed allowing investigation of the more complex temporal properties of the emergent language. By using a simple referential game, and removing extraneous modules, the findings are more generalisable and transferable to other settings.

2.1 Definitions

In referential games, agents need to identify objects from an *object space* V , which appear to them as attribute-value vectors $\mathbf{x} \in V$. To define the *object space* V , the *value space* of all possible attributes is defined as $S = \{0, 1, 2 \dots N_{val}\}$ where N_{val} is the *number of values*. The value space represents the variations each object *attribute* can have. The *object space* is

defined as $V = S_1 \times \dots \times S_N = \{(a_1, \dots, a_{N_{att}}) \mid a_i \in S_i \text{ for every } i \in \{1, \dots, N_{att}\}\}$, where N_{att} is the *number of attributes* of an object.

To give intuition to the notion of attributes and values, consider that the object shown to the sender is an abstraction of an image of a circle. The attributes of the circle could include whether the line is dashed, the colour of the line, or the colour of the background. The values are the variations of these attributes. In this example, a value of the background colour could be black, blue, or red. For example, to represent a blue, solid line circle on a red background a vector such as [blue, solid, red] could be used, which could also be represented as an integer vector, for example [2, 1, 3].

The characters available to the agents (*i.e.*, the *symbol space*) is $\omega = \{0, 1, 2 \dots N_{vocab} - 1\}$ where N_{vocab} is the *vocabulary size*. The *message space*, or the space that all messages must belong to, is defined as $\xi = \omega_1 \times \dots \times \omega_L = \{(c_1, \dots, c_L) \mid c_i \in \omega_i \text{ for every } i \in \{1, \dots, L\}\}$, where L is the maximum message length.

Combining the message and object space, the agents' language is defined as a mapping from the objects in V to messages in ξ . Finally, the exchange history, representing all messages and objects that the agents have sent/seen so far, is defined as a sequence $\tau = \{(\mathbf{m}_n, \mathbf{x}_n)\}_{n \in \{1, \dots, t\}}$ such that $\forall n, \mathbf{m}_n \in \xi \wedge \mathbf{x}_n \in V$, with t signifying the episode of the last exchange. Agent communication is defined as agents using this language to convey information about the observed object.

2.2 Temporal Logic

Temporal logic is used to formally define the behaviour of our environment, as well as an analogue for how the agents communicate. To achieve this, a form of Linear Temporal Logic (LTL) (Pnueli, 1977) called Past LTL (PLTL) (Lichtenstein et al., 1985) is employed.

LTL focuses on the connection between future and present propositions, defining operators such as “next” \circ , indicating that a given predicate or event will be true in the next step. The LTL operators can then be extended to include the temporal relationship with propositions in the past, creating PLTL. PLTL defines the operator “previously” \ominus , corresponding to the LTL operator of “next” \circ .

The “previously” PLTL operator must satisfy Equation (1), using the definitions from Maler et al. (2008), where σ refers to a behaviour of a system, the message sent by an agent, at the time t to the time that event has occurred, when the message was sent, and ϕ signifies a property, the object seen by the agent.

$$(\sigma, t) \models \ominus\phi \leftrightarrow (\sigma, t - 1) \models \phi \tag{1}$$

Additionally, the shorthand notation of \ominus^n is used, signifying that the \ominus operator is applied n episodes back. For instance, $\ominus^4\phi \leftrightarrow \ominus\ominus\ominus\ominus\phi$.

2.3 Temporal Referential Games

The temporal version of the referential games (Lewis, 1969; Lazaridou et al., 2017) is based on the “previously” (\ominus) PLTL operator.¹ At every game step s_t , the sender agent is presented

1. Code is available at <https://github.com/olipinski/TRG>

with an input object vector \mathbf{x} generated by the function $X(t, c, h_v)$, with a random *chance* parameter c , the *previous horizon* value h_v , and the current episode t .

$$X(t, c, h_v) = \begin{cases} \mathbf{x} & c = 0 \\ \ominus^{h_v} \mathbf{x} = \tau_{t-h_v} & c = 1 \end{cases} \quad (2)$$

The *previous horizon* value is uniformly sampled, taking the value of any integer in the range $[1, h]$, where h is the *previous horizon* hyperparameter. The *previous horizon* value is randomly sampled to allow agents to develop temporal references of varying temporal horizons, instead of the parameter being fixed each run. The function $X(t, c, h_v)$ selects a target object to be presented to the sender using Equation (2), either generating a new random target object or using the old target object. This choice is facilitated using the *chance* parameter c , which is sampled from a Bernoulli distribution, with $p = 0.5$. If $c = 1$ a previous target object is used, and if $c = 0$ a new target object is generated. Both c and h_v are sampled every time a target object is generated.

For example, consider an episode at $t = 4$ with the sampled parameters $c = 1$ and $h_v = 2$. Suppose the agent has observed the following targets: $[\mathbf{j}, \mathbf{k}, \mathbf{l}]$. Given that $c = 1$, further to Equation (2), the \ominus^2 (\ominus^{h_v}) target is chosen. The target sequence becomes $[\mathbf{j}, \mathbf{k}, \mathbf{l}, \mathbf{k}]$, with the target \mathbf{k} being repeated, as it was the second to last target. Now suppose that c was sampled to be $c = 0$ instead. Further to Equation (2), a random target \mathbf{a} is generated, from $\mathbf{a} \in V$. The target sequence becomes $[\mathbf{j}, \mathbf{k}, \mathbf{l}, \mathbf{a}]$.

This behaviour describes the environment *TRG*, which represents the base variant of temporal referential games, where targets are randomly generated with a 50% chance of repetition of a target from the previous horizon $[1, h]$. The *TRG Hard* variant is also used, which is a temporal referential game with the same 50% chance of a repetition, but where targets only differ in a single attribute when compared to the distractors. *TRG Hard* tests whether temporal referencing improves performance in environments where highly similar target repetitions are common. We expect that this environment will prove challenging for the agents, and so we expect an accuracy drop. However, we expect the accuracy to improve with the addition of temporal reference, as the agents should be able to overcome the target similarities by referring to the temporal relationships between the targets instead. A visual representation of the *TRG* environment is shown in Figure 1b.

Additionally, two more environments are used: *Always Same* and *Never Same*. Their purpose is to verify whether the messages that are identified as temporal references are correctly labelled. The *Always Same* environment sequentially repeats each target from a uniformly sampled subset of all possible targets ten times². Repeating the target ten times allows verification that the messages are used consistently; *i.e.*, if the agents use temporal messaging. The *Never Same* never repeats a target and goes through a subset of all possible targets in order. The *Never Same* environment is used to verify if the same messages are used for other purposes than to purely indicate that the targets are the same. In both environments, the dataset only repeats the target object, while the distractor objects are randomly generated for each object set. Sample inputs and expected outputs for these environments are provided in Appendix B.1.

2. A subset is used as the target space grows exponentially with the number of attributes and values.

The agents are also trained and evaluated in the *RG* environment, which represents the classic referential game (Lewis, 1969; Lazaridou et al., 2017), where targets are randomly generated, and *RG Hard*, which is a more difficult version of the referential games, where the target and distractors only differ in a single attribute. The *RG* environment establishes a reference performance for the agents, while *RG Hard* determines whether temporal references enhance performance in an environment where targets are harder to differentiate. Similarly to the *TRG Hard*, we expect an accuracy drop in the *RG Hard* environment.

Since the *RG*, *RG Hard*, and *Never Same* environments have almost no target repetitions, (*cf.*, Appendix B, Figure 6) we do not expect to observe the emergence of temporal references in these environments. We use *RG*, *RG Hard*, and *Never Same* to validate our results, and to provide a baseline performance on the environments usually used in emergent communication research (Boldt and Mortensen, 2024).

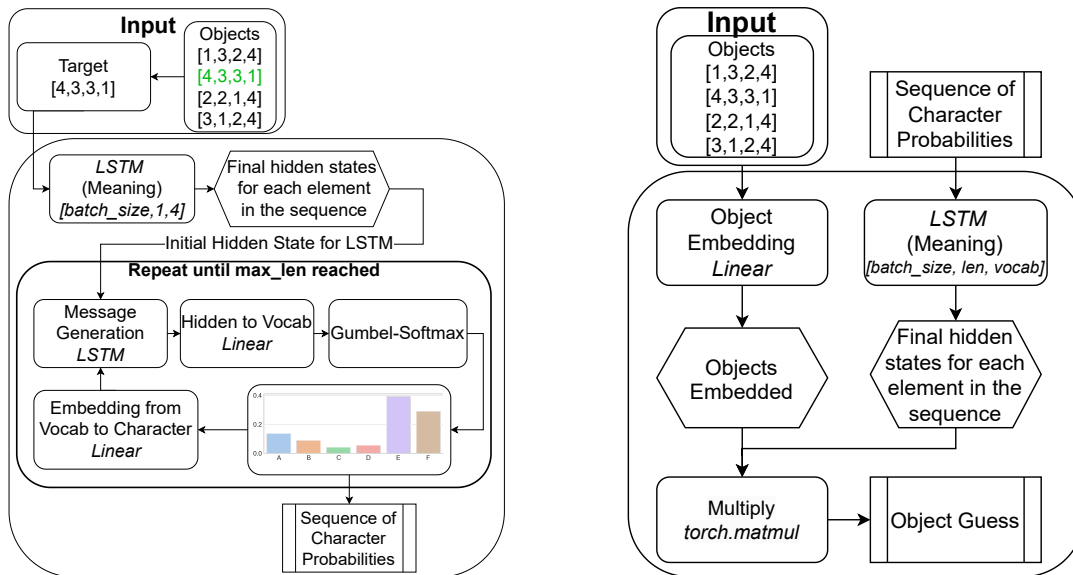
3 Architectures

In emergent communication, both sender and receiver agents are typically built around a single recurrent neural network (Kharitonov et al., 2019). In this paper, these standard agent architectures, based on an LSTM (Hochreiter and Schmidhuber, 1997), are compared to temporal LSTM architectures, which use a different batching strategy. The *Base* agent, used as a baseline, is the commonly used LSTM-based EGG agents (Hochreiter and Schmidhuber, 1997; Kharitonov et al., 2019). Our two novel architectures, the *Temporal* and *TemporalR* agents, feature a sequentially batched LSTM Hochreiter and Schmidhuber (1997). This additional module allows the agents to gather information about the sequence of object itself, instead of the regular LSTM, as used in EGG (Kharitonov et al., 2019), which processes all objects in parallel. While the *Temporal* agents use just the sequential LSTM to process their input, the *TemporalR* agents combine both the *Base* and *Temporal* approaches, combining the outputs of a regular LSTM, together with the sequentially batched LSTM. This allows the *TemporalR* agents to process the information that may be present in the objects themselves, as well as the order of their appearances, without needing to store this information in a single LSTM hidden state.

While many architectures may work for processing temporal information within datasets, we opt for a distinct batching strategy for two key reasons. Firstly, it entails the least modification to the *Base* agent design, facilitating direct comparisons between the two architectures and enabling straightforward application of our architectural modifications to other contexts. Secondly, it offers a straightforward framework for examining the emergence of temporal references. Although our experiments initially involved more complex architectures, including attention-based agents, we observed no significant differences in any metrics from those of LSTM-based networks. Consequently, our focus in this study remains on LSTM-based agents.

3.1 Base Agent

In common with other approaches (Kharitonov et al., 2019; Chaabouni et al., 2019; Auersperger and Pecina, 2022), each of the *Base* sender and receiver agents are constructed around a single LSTM (Hochreiter and Schmidhuber, 1997). First, the sender’s LSTM (Figure 2a) receives each target and distractor set individually, processing each object separately. The


 (a) The *Base* LSTM sender architecture.

 (b) The *Base* LSTM receiver architecture.

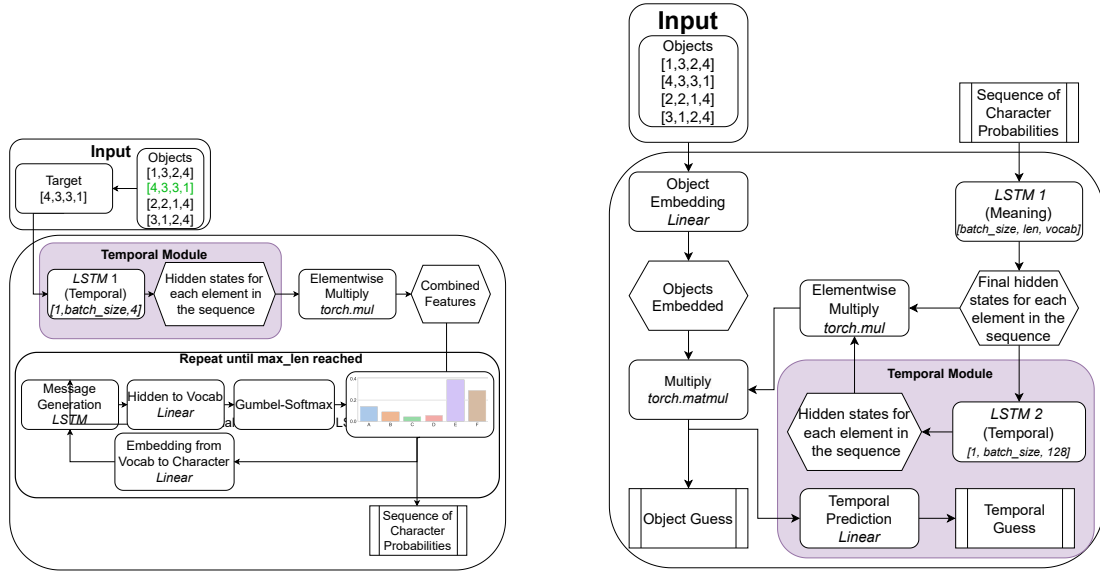
 Figure 2: The *Base* LSTM sender and receiver architectures.

result is the initial hidden state for the message generation LSTM. For message generation, the same method is followed as used in previous work (Kharitonov et al., 2019), and messages are generated character by character, using the Gumbel-Softmax trick (Jang et al., 2017). These messages are then passed to the receiver, an overview of which is shown in Figure 2b. The receiver’s architecture contains an object embedding linear layer and a message processing LSTM, similar to the most commonly used architecture from the EGG framework (Kharitonov et al., 2019). In the receiver agent, a hidden state is computed for each message by the LSTM. This output is combined with the output of the object embedding linear layer to create the referential game object prediction.

3.2 Temporal Agent

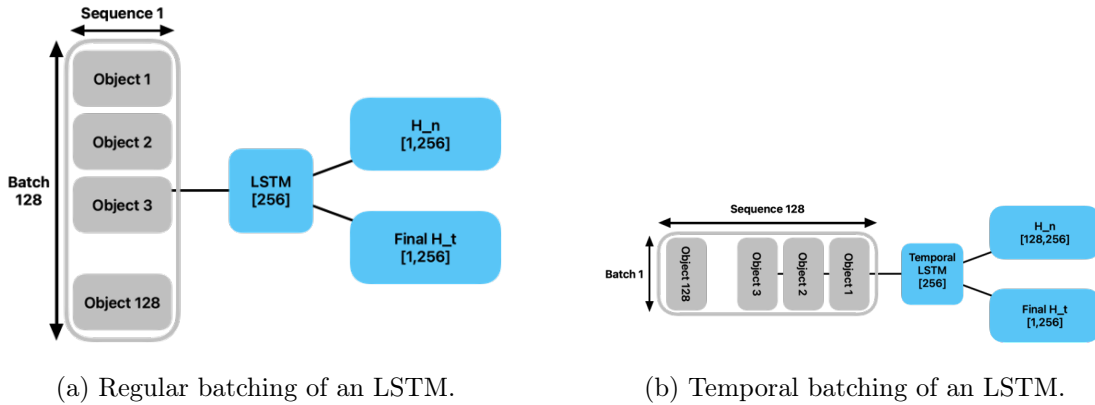
For the *Temporal* agent, a sequential LSTM module is introduced in both the sender and receiver networks (Figure 3). This additional LSTM is batched with a sequence over the whole training input, similar to the sequential learning of language in humans (Christiansen and Kirby, 2003). By including this sequential LSTM, the sender and the receiver are able to develop a more temporally focused understanding. This ability to process temporal relationships is proposed to allow the agents to represent the entire object sequence within the LSTM hidden state. Since it does not require reward shaping approaches or architectures specifically designed for referential games, this addition is also a scalable and general approach to allowing temporal references to develop. A different batching strategy can be applied to any environment and agent.

Assume the sender LSTM expects an input of the form $[batch_size, seq_len, N_{att}]$. Let $batch_size = 128$, and $N_{att} = 6$. A batch of shape $[128, 1, 6]$ is then created, obtaining 128



(a) The *Temporal LSTM* sender architecture. (b) The *Temporal LSTM* receiver architecture.

Figure 3: The *Temporal LSTM* sender and receiver architectures, with the temporal modules highlighted in purple.



(a) Regular batching of an LSTM. (b) Temporal batching of an LSTM.

Figure 4: Examples of regular and temporal batching strategies.

objects of size 6, with sequence length 1 (Kharitonov et al., 2019). The sequential LSTM instead receives a batch of shape $[1, 128, 6]$, or a sequence of 128 objects of size 6. This allows the sequential LSTM to process all objects one after another to create temporal understanding, a visual representation is in Figure 4.

Additionally, the temporal prediction layer and the sequential LSTM are also used in the receiver agent. First, a hidden state is computed for each message using the regularly batched LSTM. Then, the sequential LSTM processes each of the regularly batched LSTM’s hidden states to build a temporal understanding of the sender’s messages. The combined information from both LSTMs and the object is also used in the temporal prediction layer,

which allows the agent to signify whether an object is the same as a previously seen object, up to the previous horizon h . This is implemented as a single linear layer, which outputs the temporal label prediction.

The temporal label used in this prediction only considers the previous horizon h ; otherwise, it defaults to 0. For example, assume an object has been repeated in the current episode and last appeared 5 episodes ago. If the previous horizon, h , is 8, the label assigned to this object would be 5, as 5 past episodes are still within the horizon, *i.e.*, $5 \leq h$. However, if h is 4, the label would be 0, as the episode lies outside the previous horizon, *i.e.*, $4 \geq h$.

This predictive ability is combined with an additional term in the loss function, which together form a **temporal prediction loss**. The agent’s loss function can be formulated as $L_t = L_{rg} + L_{tp}$. The L_{rg} component is the referential game loss between the receiver guess and the sender target label, using cross entropy. L_{tp} is the temporal prediction loss, which is implemented using cross entropy between the labels of when an object has last appeared, and the receiver’s prediction of that label. Agents that include this loss perform an additional task, which corresponds to correctly identifying which two outputs are the same. The goal of this loss is to improve the likelihood of an agent developing temporal references by increasing the focus on these relationships. Analysis of how the presence of this explicit loss impacts the development of temporal references is provided in Section 5.

3.3 TemporalR Agent

The *TemporalR* agent combines the *Base* and the *Temporal* architectures. The sequential LSTM from the *Temporal* agent is added to the *Base* architecture, merging both the sequential understanding from the temporal module, with the parallel understanding of the target objects from the regularly batched LSTM. The hidden states of both LSTMs are combined through an elementwise multiplication and fed into the message generation LSTM. The receiver agent is the same as the *Temporal* receiver, and includes the temporal prediction module.

4 Metrics

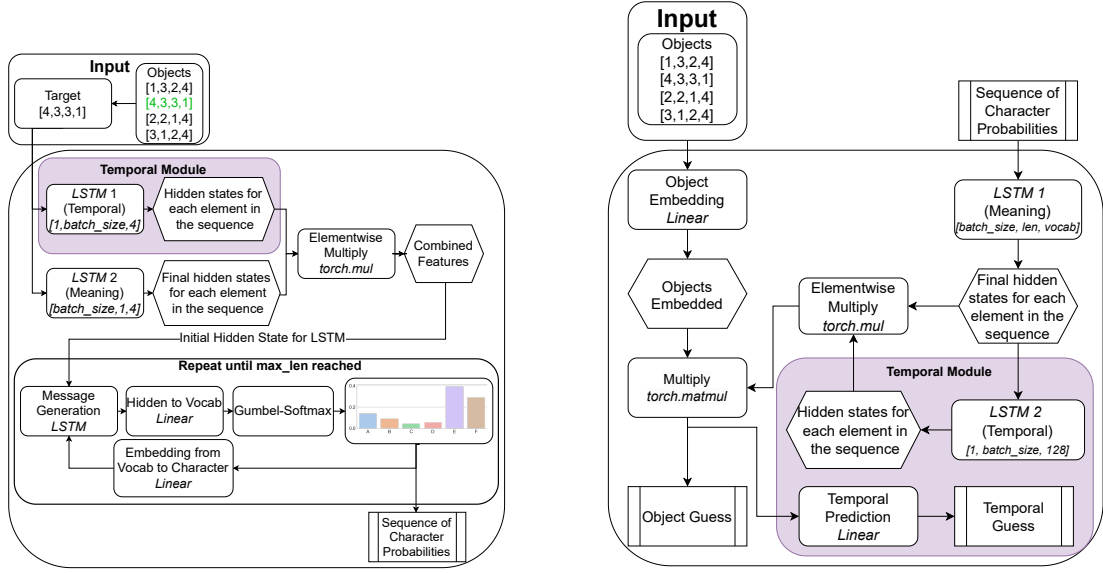
4.1 Temporality Metric

To evaluate the development of temporal references, we propose a new metric, M_{\ominus^n} , which measures how often a given message has been used as the “previous” operator in prior communication. Given an exchange history (the sequence of objects shown to the sender and messages sent to the receiver), τ , it checks when an object has been repeated within a given horizon h_v , and records the corresponding message sent to describe that object.

Let $C_{\mathbf{m}\ominus^n}$ count the times the message \mathbf{m} has been sent together with a repeated object for $h_v = n$:

$$C_{\mathbf{m}\ominus^n} = \sum_{j=1}^t \mathbb{I}(\mathbf{m}_j = \mathbf{m} \wedge \text{objectSame}(\mathbf{x}_j, n)) \quad (3)$$

where $\mathbb{I}(\cdot)$ is the indicator function that returns 1 if the condition is true and 0 otherwise, and $\text{objectSame}(\mathbf{x}_j, n)$ is a function that evaluates to true if the object \mathbf{x}_j is the same as the object n episodes ago.



(a) The *TemporalR* LSTM sender architecture. (b) The *TemporalR* LSTM receiver architecture.

Figure 5: The *TemporalR* LSTM sender and receiver architectures, with the temporal modules highlighted in purple.

Let \mathcal{T}_m denote the total count of times the message m has been used:

$$\mathcal{T}_m = \sum_{j=1}^t \mathbb{I}(m_j = m) \quad (4)$$

where $\mathbb{I}(\cdot)$ is an indicator function selecting the message m in the exchange history τ .

The percentage of previous messages that are the same as m can then be calculated using $M_{\ominus^n}(m)$:

$$M_{\ominus^n}(m) = \frac{C_m \ominus^n}{\mathcal{T}_m} \times 100 \quad (5)$$

The objective of the $M_{\ominus^n}(m)$ metric is to measure if the message can give reference to a previous episode; *e.g.*, if a message is used similarly to the sentence ‘‘The car I can see is the same colour as the one mentioned two sentences ago’’. More formally, assume a target object sequence of $[x, y, z, y, y, y, x]$. Each vector, x, y, z , represents an object belonging to the same arbitrary V . In this example, there is only one object repeating: y . We can then consider three message sequences: $[m_1, m_2, m_3, m_2, m_4, m_4, m_1]$, $[m_1, m_2, m_3, m_4, m_4, m_4, m_1]$ and $[m_1, m_2, m_3, m_2, m_2, m_2, m_1]$, with each m_n belonging to the same arbitrary ξ and calculate the metric \ominus^1 .

There are two repetitions in the sequence of objects: the second and third y following the sequence of $[x, y, z, y]$. In the first example message sequence, the message m_4 has been sent and so $C_{m_4} \ominus^1 = 2$, for both of the repetitions. The total use of m_4 is $\mathcal{T}_{m_4} = 2$. Calculating the metric $M_{\ominus^1}(m_4) = 2/2 \times 100 = 100\%$ gives 100% for the use of m_4 as a \ominus^1 operator. The result of 100% indicates that this message is used exclusively as a \ominus^1 operator.

In the second message sequence, \mathbf{m}_4 has also been used for the initial observation of the object. This means that $\mathcal{T}_{\mathbf{m}_4} = 3$, while $C_{\mathbf{m}_4} \ominus^1 = 2$, $M_{\ominus^1}(\mathbf{m}_4) = 2/3 \times 100 = 66\%$, which shows the message being used as \ominus^1 66% of the time.

Lastly, the simplest case of a message describing an object exactly. Following the previous examples, $\mathcal{T}_{\mathbf{m}_2} = 4$, with $C_{\mathbf{m}_2} \ominus^1 = 2$. This message would then be classed as 50% \ominus^1 usage, $M_{\ominus^1}(\mathbf{m}_2) = 2/4 \times 100 = 50\%$. A non-100% result indicates that the message is not used exclusively as a \ominus^1 operator.

4.2 Compositionality Metrics

The emergent languages are also analysed in terms of their compositionality scores, using the **topographic similarity** metric (Brighton and Kirby, 2006), commonly employed in emergent communication. Topographic similarity measures the Spearman Rank correlation (Spearman, 1904) between the distances of messages and objects in their respective spaces. For example, a message describing a “blue circle” should be closer to “blue triangle”, than to “red square”, given the language is compositional.

The languages are also evaluated using metrics which account for languages where the symbols themselves carry all the information: **posdis**, which use the positional information of individual characters, and **bosdis**, for permutation invariant languages, (Chaabouni et al., 2020). **Posdis** intuitively measures if, for example, the first symbol always refers to a property of the object, such as in the English phrases “blue circle” or “red square”, versus “circle blue” or “square red”. **Bosdis** measures whether a symbol carries all the information **independent** of the position of this symbol, such as in the English conjunctions example from Chaabouni et al. (2020), “dogs and cats” and “cats and dogs”, where both constructions are valid and convey the same information.

5 Experiments

5.1 Hypotheses

To study the impact of the architecture, as well as the external and internal pressures of the agents, we propose three hypotheses to guide our experiments:

Hypothesis 1 (H1) All agents can develop some form of temporal references, with agents that include the temporal prediction loss more likely to do so.

Hypothesis 2 (H2) Temporal references will increase the agent’s performance in environments which include temporal relationships.

Hypothesis 3 (H3) No temporal references will be detected with the M_{\ominus^n} metric in environments where there are no temporal relationships.

Hypothesis 1 is investigated by using multiple agent types and applying a temporal prediction loss. Hypothesis 2 is analysed by using two environments, TRG and TRG Hard, where temporal relationships are explicitly introduced. We then compare the performance of agents which develop temporal references, to those which do not to determine the impact of temporal references on the task accuracy. We include all evaluation environments, including those where there are no target repetitions when evaluating the M_{\ominus^n} to validate Hypothesis 3, which acts as a sanity check.

5.2 Agent Training

The following architectures are trained and evaluated:

- Base** The same as the EGG (Kharitonov et al., 2019) agents, used as a baseline for comparisons (Section 3.1);
- Temporal** The base learner with the sequential LSTM **instead** of the regularly batched LSTM (Section 3.2); and
- TemporalR** The base learner with the regularly batched LSTM **and** the sequential LSTM (Section 3.3)

Each agent type is additionally trained with and without the **temporal prediction loss**. The agents that include the temporal prediction loss have an explicit reward to develop temporal understanding. There is no additional pressure to develop temporal references for agents that do not include the temporal prediction loss, except for the possibility of increased performance on the referential task. The aim of the additional loss is to investigate if it would aid in the temporal reference emergence, or if it improves agent performance.

The emergence of temporal references is defined as the appearance of messages which reach 100% on our M_{\ominus^n} metric. We employ a 100% threshold to ensure that only messages consistently used as temporal references are considered, thereby mitigating the influence of chance repetitions on our results. Consequently, the M_{\ominus^n} metric is expected to reach 100% for all agents.

All agent types were trained for the same number of epochs and on the same environments during each run. Agent pairs are trained in either the RG or TRG environment. Evaluation of the agents is performed after the training has finished. Each agent pair is assessed in six different environments: Always Same, Never Same, RG, RG Hard, TRG and TRG Hard. The target objects are uniformly sampled from the object space V in all environments. Each possible configuration was run ten times, with randomised seeds between runs for both the agents and the datasets. Appendix A provides further details.

5.3 Significance Analysis

The underlying distribution of each network type is analysed, using the Kruskal-Wallis H-test (Kruskal and Wallis, 1952), as scores are not guaranteed to be distributed normally, which violates the parametric ANOVA assumption. Conover-Iman (Conover and Iman, 1979) post-hoc analysis is performed, with Holm-Bonferroni (Holm, 1979) corrections applied, to verify which of the different network types differ significantly from each other. Using these methods, all results reported in the following sections have been verified to be statistically significant, with $p < 0.05$. The detailed results of the significance analyses are shown in the supplemental material.

5.4 Task Accuracy

All agents achieve high task accuracy, with all achieving over 95% in the Referential Games (RG) environment. Both Hard variants (*i.e.*, RG Hard and TRG Hard) present a challenge to the agents. All agents perform significantly worse in these two evaluation environments, achieving approximately 72% accuracy on average for the RG Hard environment, and 85% accuracy for the TRG Hard environment. We observe no increase in the task accuracy for

the agents which develop temporal references, proving H2 incorrect. We provide a discussion of the possible reasons behind this in Section 6. The detailed accuracy distributions are provided in Appendix D.

5.5 Temporality Sanity Check

In line with H3, the values of M_{\ominus^n} for the Never Same, RG, and RG Hard environments consistently register at 0%. These results reduce the likelihood of significant issues with the M_{\ominus^n} metric, given that the probability of target repetition in these environments is near zero. Since the results remain constant and at 0% for these environments, they are omitted from the subsequent sections for brevity. Detailed results for these environments are available in both Appendices D and E and supplemental material.

5.6 Temporality Analysis

Table 1 illustrates the M_{\ominus^4} metric values, referring to an observation four messages in the past, of all agent types over the evaluation environments (*cf.*, Sections 4 and 5.2), where $M_{\ominus^4} \geq 0\%$.³

Table 1 indicates that the temporally focused processing of the input data makes the agents predetermined to develop temporal references. Only the sequential LSTM (*Temporal* and *TemporalR*) agents, are capable of producing temporal references. Temporal references emerge in these networks, regardless of the training dataset. Even in a regular environment, without additional pressures, temporal references are advantageous. No messages in the *Base* architectures are used 100% of the time for \ominus^4 , irrespective of the dataset they have been trained on. The temporal prediction loss is not enough, and that the ability to process observations temporally is the key factor to the emergence of temporal references. These results partially confirm H1, indicating that all agents capable of explicitly processing temporal relationships develop temporal references and that no additional pressures are required. While we expected that the additional temporal prediction loss would improve the development of temporal references, this analysis indicates that it is not sufficient, nor necessary.

Additionally, messages that are used for \ominus^4 have a high chance of being correct, with most averaging above 90% **correctness**. **Correctness** refers to whether the receiver agent correctly guessed the target object after receiving the message. A detailed overview of the distribution of message correctness is provided in the supplemental material.

Most messages are used only in the context of the current observations, with *Temporal* and *TemporalR* networks using a more specialised subset of messages to refer to the temporal relationships. Only *Temporal* and *TemporalR* variants develop messages that reach 100% on the M_{\ominus^4} metric. The distribution also suggests that these messages could be a more efficient way of describing objects, as the number of temporal messages is relatively small. Since only a small number of messages are needed for the temporal references, they could be used more frequently. This message specialisation, combined with a linguistic parsimony pressure (Rita et al., 2020), could lead to a more efficient way of describing an object: sending the object

3. The value of 4 is chosen arbitrarily, to lie in the middle of the explored range of h . More detailed analysis from $h_v = 1$ to $h_v = 8$ is provided in the supplemental material

Network	Loss	Training Env	AS	TRG	TRG Hard
Base	Reg	RG	60%	85%	85%
Base	Reg	TRG	60%	85%	85%
Base	Reg+T	RG	60%	85%	85%
Base	Reg+T	TRG	60%	85%	85%
Temporal	Reg	RG	100%	100%	100%
Temporal	Reg	TRG	100%	100%	100%
Temporal	Reg+T	RG	100%	100%	100%
Temporal	Reg+T	TRG	100%	100%	100%
TemporalR	Reg	RG	100%	100%	100%
TemporalR	Reg	TRG	100%	100%	100%
TemporalR	Reg+T	RG	100%	100%	100%
TemporalR	Reg+T	TRG	100%	100%	100%

Table 1: Maximum value of the M_{\ominus^4} metric for each network/loss/training environment combination. “AS” is Always Same, “RG” is the regular Reference Game environment, “TRG” is the Temporal Reference Game, and “TRG Hard” is TRG with the target differing in a single attribute with respect to the distractors.

properties requires more bandwidth than sending only the time step the object last appeared. A detailed breakdown of the messages used is provided in the supplemental material.

The percentage of networks that develop temporal messaging is shown in Table 2. The percentages shown are absolute values, calculated by taking the total number of runs and checking whether at least one message has reached $M_{\ominus^n} = 100\%$ for each run. That number of runs is divided by the total number of runs of the corresponding configuration to arrive at the quantities in Table 2.

The *Temporal* and *TemporalR* network variants reach over 96% of runs that have converged to a strategy which uses at least one message as the \ominus^n operator. In contrast, the *Base* networks never achieve such a distinction. However, some runs have not converged to a temporal strategy in the case of the *TemporalR* network. These instances account for only 3% of the total number of runs, and the differences are **not** statistically significant from the *Temporal* network, showing that the emergence of temporal references is still very likely, if somewhat dependent on the network initialisation. These results indicate that the ability to build a temporally focused representation of the input data is the deciding factor in the emergence of temporal references.

When increasing the number of target repetitions in a dataset, the use of temporal messages increases. As the repetition chance p increases, the percentage of messages that are used for \ominus^n increases for all agent variants. On average, *Base* networks demonstrate the same chance of using a message for \ominus^n as the dataset repetition chance. This means that while the percentage increases, it is only due to the increase in the repetition chance. If a dataset contains 75% repetitions, on average, each message will be used as an accidental \ominus^n 75% of the time. For example, if the language does not have temporal references and uses a given message to describe an object, this message will be repeated every time this object appears. This means that for every repetition, the message could be considered a

Table 2: Percentage of networks that develop temporal messages.

Network Type	Loss Type	Percentage
Base	Regular loss	0%
Base	Regular + Temporal loss	0%
Temporal	Regular loss	100%
Temporal	Regular + Temporal loss	100%
TemporalR	Regular loss	98.66%
TemporalR	Regular + Temporal loss	97%

message indicating a *previous* episode, whereas, in reality, it is just a description of the object. In contrast to the *Base* networks, for *Temporal* and *TemporalR* networks, the average percentage does reach 100%. This means that messages the agents designate for \ominus^n are used more often than the repetition chance.

5.7 Compositionality Analysis

All agents create compositional languages with varying degrees of structure, which shows that learning to use temporal references does not negatively impact compositionality. All agents reach values between 0.1 and 0.2 (the higher, the more compositional the language is) on the topographic similarity metric (Brighton and Kirby, 2006; Rita et al., 2022b), where a score of 0.4 has been considered high in previous research (Rita et al., 2022b). We provide a visual representation of the topographic similarity scores in Appendix E. These results indicate that temporal references have no negative effect on the languages’ compositionality, showing that their emergence does not necessitate a trade-off in the possible generalisation ability of the emergent language (Auersperger and Pecina, 2022).

The differences between the **posdis** and **bosdis** distributions for each network type are not statistically significant. Therefore, the differences in the **posdis** and **bosdis** metrics across network types could be due to random fluctuations in the score distribution.

5.8 Generalisation Analysis

Analysing the development of temporal references, we observe the emergence of messages being used by the agents to describe the previous $h_v = 4$ episodes. As an example of such behaviour, in one of the runs where the agents were trained in the *TemporalR* configuration, the message [25, 6, 9, 3, 2] was consistently used as a \ominus^1 operator. When the agents were evaluated in the Always Same environment, they used this message only when the target objects were repeating, while also being used exclusively for twelve distinct objects. For a total of 10 repetitions of each object, this message was utilised nine times, indicating that the only time a different message was sent was when the object appeared for the first time. For example, when the object [4, 2, 3, 6, 5, 8, 8, 4] appeared for the first time, a message [25, 6, 17, 9, 9] was sent, and subsequently the temporal message was used. This shows that temporal messages aid generalisation. A message that has been developed in a different training environment, in this case TRG, can be subsequently used during evaluation, even if the targets are not shared between the two environments.

6 Discussion

The results indicate that no explicit pressures are required for temporal messages to emerge, unlike increasing linguistic parsimony where additional losses are needed (Rita et al., 2020; Kalinowska et al., 2022). We show that the incentives are already present in datasets that are *not* altered to increase the number of repetitions occurring. Temporal references therefore emerge naturally, as long as the agents are able to build a temporal understanding of the data, such as with the sequential LSTM in the *Temporal* and *TemporalR* agents. This allows temporal references to emerge in any communication settings if a suitable architecture is used. This could provide greater bandwidth efficiency by allowing agents to use shorter messages for events that happen often, when combined with other linguistic parsimony approaches (Rita et al., 2020; Chaabouni et al., 2019).

The emergence of temporal references only through architectural changes could also point towards additional insights in terms of modelling human language evolution using EC (Galke et al., 2022). These architectural approaches to the emergence of temporal references could be viewed as analogous to sequential learning in natural language (Christiansen and Kirby, 2003), as we learn to encode and represent elements in temporal sequences.

6.1 Accuracy

As expected, both the RG Hard and the TRG Hard environments posed a challenge, presenting a significant accuracy drop. In the case of the *Temporal*, *TemporalR* agents, we hypothesised the emergence of temporal references to provide an advantage, increasing the agents’ accuracy (Section 5.1). While there indeed is a small increase in accuracy in the TRG Hard environment, it is not attributable to temporal references (*cf.*, Appendix D). This is because we observe the same increase for the *Base* agents, which do not develop temporal references. We conclude that the increase is due to increased object repetition, making the task slightly easier.

A possible cause for the lack of accuracy increase for agents which develop temporal references might be the perceptual similarities between the highly similar distractor objects. This makes the task of discerning the difference between these objects becoming too difficult for the receiver. Alternatively, if the receiver struggled to correctly identify an object the first time it has observed it, the additional information that temporal references would offer would not be enough. The receiver would not know what the correct choice was for the previous timesteps.

Additionally, networks that have been trained with the temporal loss **and** on the temporally focused dataset, perform slightly worse, by about 1%. The reason for the accuracy drop could lie in too much pressure on the temporal aspects of the dataset. Because of the additional loss, agents can increase their rewards by only focusing on creating temporal messages, without learning a general communication protocol. This then leads to overfitting the training dataset, where they can rely on both their mostly temporal language and their memory of the object sequences, instead of communicating about the object attributes. Consequently, we observe a decline in performance on the evaluation dataset.

6.2 Compositionality

We hypothesise the effect of the temporal loss on the topographic similarity scores (we do not discuss the **posdis** and **bosdis** scores, as there are no statistically significant differences) is similar to that of the task accuracy. Since the agents focus on the temporal aspects of the task and dataset more, they develop less general languages, leading to lower compositionality scores. We do not believe the low compositionality scores are related to the simplicity of the dataset, being composed of integer vectors, since other works in similar settings achieve higher topographic similarity scores (Chaabouni et al., 2020; Rita et al., 2022b).

7 Limitations

All reported compositionality scores could be negatively affected by the presence of temporal references. Temporal messages can be compositional, but they would not refer to a specific object, and so topographic similarity would not be able to identify them correctly. Similarly, since **posdis** and **bosdis** also rely on the mappings between the messages and the dataset, instead of the temporal relationships captured by the temporal references, they could also be inaccurately lowered by their presence. Since temporal references, even if they were compositional, do not map directly to object properties in the dataset, they would be counted as non-compositional messages, therefore lowering the values of the evaluated metrics. This could be the reason for the lower values observed in our experiments when compared to previous research (Rita et al., 2022b).

8 Conclusion

Emergent communication has been studied extensively, considering many aspects of emergent languages, such as efficiency (Rita et al., 2020; Chaabouni et al., 2019), compositionality (Auersperger and Pecina, 2022), generalisation (Chaabouni et al., 2020) and population dynamics (Chaabouni et al., 2022; Rita et al., 2022a). Yet, there has been no investigation into learning and communicating temporal relationships. Discussing past observations is vital to communication, saving bandwidth by avoiding repeating information and allowing for easier experience sharing.

This paper provides a first exploration of such emergent languages, including addressing the fundamental questions of when they could develop and what is required for their emergence. We present a set of environments that are designed to facilitate investigation into how agents might create such references. We use the conventional agent architecture for emergent communication (Kharitonov et al., 2019) as a baseline and explore both temporal loss and alternative architectures that may endow agents with the ability to learn temporal relationships. We show that architectural change is necessary for temporal references to emerge, and demonstrate that temporal prediction loss is neither sufficient for their emergence, nor does it improve the emergent language.

Acknowledgments and Disclosure of Funding

This work was supported by the UK Research and Innovation Centre for Doctoral Training in Machine Intelligence for Nano-electronic Devices and Systems [EP/S024298/1]. The authors would like to thank Lloyd’s Register Foundation for their support, and acknowledge the use of the IRIDIS High-Performance Computing Facility, and associated support services at the University of Southampton, in the completion of this work.

References

- Michal Auersperger and Pavel Pecina. Defending compositionality in emergent languages. In *Proceedings of the 2022 Conference of the NAACL: Human Language Technologies: Student Research Workshop*, pages 285–291, 2022.
- Lukas Biewald. Experiment Tracking with Weights and Biases, 2020.
- Brendon Boldt and David R. Mortensen. A Review of the Applications of Deep Learning-Based Emergent Communication. *Transactions on Machine Learning Research*, 2024. ISSN 2835-8856.
- Tom Bosc. Varying meaning complexity to explain and measure compositionality. In *Emergent Communication Workshop at ICLR 2022*, 2022.
- Nicolo’ Brandizzi, Davide Grossi, and Luca Iocchi. RLupus: Cooperation through emergent communication in The Werewolf social deduction game. *Intelligenza Artificiale*, 15(2): 55–70, 2021.
- Henry Brighton and Simon Kirby. Understanding Linguistic Evolution by Visualizing the Emergence of Topographic Mappings. *Artificial Life*, 12(2):229–242, 2006. ISSN 1064-5462.
- Rahma Chaabouni, Eugene Kharitonov, Emmanuel Dupoux, and Marco Baroni. Anti-efficient encoding in emergent communication. In *Proceedings of NeurIPS*, 2019.
- Rahma Chaabouni, Eugene Kharitonov, Diane Bouchacourt, Emmanuel Dupoux, and Marco Baroni. Compositionality and generalization in emergent languages. In *Proceedings of ACL*, pages 4427–4442, 2020.
- Rahma Chaabouni, Florian Strub, Florent Alché, Eugene Tarassov, Corentin Tallec, Elnaz Davoodi, Kory Wallace Mathewson, Olivier Tieleman, Angeliki Lazaridou, and Bilal Piot. Emergent communication at scale. In *Proceedings of ICLR*, 2022.
- Morten H. Christiansen and Simon Kirby. Language evolution: consensus and controversies. *Trends in Cognitive Sciences*, 7(7):300–307, 2003.
- WJ Conover and RL Iman. On multiple-comparisons procedures. Technical report, Los Alamos National Lab, 1979.
- William Falcon and The PyTorch Lightning Team. PyTorch Lightning, 2019.

- Lukas Galke, Yoav Ram, and Limor Raviv. Emergent Communication for Understanding Human Language Evolution: What’s Missing? In *Emergent Communication Workshop at ICLR 2022*, 2022.
- Sepp Hochreiter and Jürgen Schmidhuber. Long Short-Term Memory. *Neural Computation*, 9(8):1735–1780, 1997.
- Sture Holm. A Simple Sequentially Rejective Multiple Test Procedure. *Scandinavian Journal of Statistics*, 6(2):65–70, 1979.
- David A. Huffman. A Method for the Construction of Minimum-Redundancy Codes. *Proceedings of the IRE*, 40(9):1098–1101, 1952.
- Eric Jang, Shixiang Gu, and Ben Poole. Categorical reparameterization with gumbel-softmax. In *Proceedings of ICLR*, 2017.
- Aleksandra Kalinowska, Elnaz Davoodi, Florian Strub, Kory Mathewson, Todd Murphey, and Patrick Pilarski. Situated Communication: A Solution to Over-communication between Artificial Agents. In *Emergent Communication Workshop at ICLR 2022*, 2022.
- Yipeng Kang, Tonghan Wang, and Gerard de Melo. Incorporating pragmatic reasoning communication into emergent language. In *Proceedings of NeurIPS*, 2020.
- Eugene Kharitonov, Rahma Chaabouni, Diane Bouchacourt, and Marco Baroni. EGG: a toolkit for research on emergence of lanGuage in games. In *Proceedings of EMNLP*, 2019.
- Diederik P. Kingma and Jimmy Ba. Adam: A method for stochastic optimization. In *Proceedings of ICLR*, 2015.
- Donald E Knuth. Dynamic huffman coding. *Journal of Algorithms*, 6(2):163–180, 1985.
- Kavya Kopparapu, Edgar A. Duéñez-Guzmán, Jayd Matyas, Alexander Sasha Vezhnevets, John P. Agapiou, Kevin R. McKee, Richard Everett, Janusz Marecki, Joel Z. Leibo, and Thore Graepel. Hidden Agenda: a Social Deduction Game with Diverse Learned Equilibria. *ArXiv preprint*, 2022.
- William H. Kruskal and W. Allen Wallis. Use of Ranks in One-Criterion Variance Analysis. *Journal of the American Statistical Association*, 47(260):583–621, 1952.
- Angeliki Lazaridou and Marco Baroni. Emergent Multi-Agent Communication in the Deep Learning Era. *ArXiv preprint*, abs/2006.02419, 2020.
- Angeliki Lazaridou, Alexander Peysakhovich, and Marco Baroni. Multi-agent cooperation and the emergence of (natural) language. In *Proceedings of ICLR*, 2017.
- Angeliki Lazaridou, Karl Moritz Hermann, Karl Tuyls, and Stephen Clark. Emergence of linguistic communication from referential games with symbolic and pixel input. In *Proceedings of ICLR*, 2018.
- David Kellogg Lewis. *Convention: A Philosophical Study*. Cambridge, MA, USA: Wiley-Blackwell, 1969.

- Orna Lichtenstein, Amir Pnueli, and Lenore Zuck. The glory of the past. In *Workshop on Logic of Programs*, pages 196–218. Springer, 1985.
- Olaf Lipinski, Adam Sobey, Federico Cerutti, and Timothy J. Norman. Emergent Password Signalling in the Game of Werewolf. In *Emergent Communication Workshop at ICLR 2022*, 2022.
- Oded Maler, Dejan Nickovic, and Amir Pnueli. Checking Temporal Properties of Discrete, Timed and Continuous Behaviors. In *Pillars of Computer Science: Essays Dedicated to Boris (Boaz) Trakhtenbrot on the Occasion of His 85th Birthday*, Lecture Notes in Computer Science, pages 475–505. Springer, 2008.
- Amir Pnueli. The temporal logic of programs. In *18th Annual Symposium on Foundations of Computer Science*, pages 46–57, 1977.
- Mathieu Rita, Rahma Chaabouni, and Emmanuel Dupoux. “LazImpa”: Lazy and impatient neural agents learn to communicate efficiently. In *Proceedings of the CoNLL*, 2020.
- Mathieu Rita, Florian Strub, Jean-Bastien Grill, Olivier Pietquin, and Emmanuel Dupoux. On the role of population heterogeneity in emergent communication. In *Proceedings of ICLR*, 2022a.
- Mathieu Rita, Corentin Tallec, Paul Michel, Jean-Bastien Grill, Olivier Pietquin, Emmanuel Dupoux, and Florian Strub. Emergent Communication: Generalization and Overfitting in Lewis Games. In *Proceedings of NeurIPS*, 2022b.
- C. Spearman. The Proof and Measurement of Association between Two Things. *The American Journal of Psychology*, 15(1):72–101, 1904.
- Valentin Taillandier, Dieuwke Hupkes, Benoît Sagot, Emmanuel Dupoux, and Paul Michel. Neural Agents Struggle to Take Turns in Bidirectional Emergent Communication. In *Proceedings of ICLR*, 2023.
- Ryo Ueda and Koki Washio. On the relationship between Zipf’s law of abbreviation and interfering noise in emergent languages. In *Proceedings of ACL*, pages 60–70, 2021.
- Ryo Ueda, Taiga Ishii, Koki Washio, and Yusuke Miyao. Categorical Grammar Induction as a Compositionality Measure for Emergent Languages in Signaling Games. In *Emergent Communication Workshop at ICLR 2022*, 2022.
- Jeffrey Scott Vitter. Design and analysis of dynamic Huffman codes. *Journal of the ACM*, 34(4):825–845, 1987.
- George Kingsley Zipf. *Human behavior and the principle of least effort*. 1949.

Appendix A. Training Details

Our agents were trained using PyTorch Lightning (Falcon and The PyTorch Lightning Team, 2019) using the Adam optimizer (Kingma and Ba, 2015), with experiment tracking done via Weights & Biases (Biewald, 2020). We provide our grid search parameters per network and per training environment in Table 3. We ran a manual grid search over these parameters for each network and training dataset combination, where the networks were *Base*, *Temporal*, *TemporalR* and the training datasets were Referential Games or Temporal Referential Games. Each trained network was then evaluated on the six available environments: Always Same, Never Same, Referential Games, Temporal Referential Games, Hard Referential Games, and Hard Temporal Referential Games. Running the grid search for one iteration, with the value of repetition chance fixed, took approximately 28 hours, using the compute resources in Table 4.

Table 3: Grid Search Parameters

Parameter	Value
Epochs	[600]
Optimizer	Adam
Learning Rate α	0.001
Number of Objects in Dataset	[20 000]
Number of Distractors	[10]
Number of Attributes N_{att}	[8]
Number of Values N_{val}	[8]
Temporal Prediction Loss Present	[True, False]
Length Penalty	[0]
Maximum Message Length L	[5]
Vocabulary Size N_{vocab}	[26]
Repetition Chance (p)	[0.25, 0.5, 0.75]
Previous Horizon h	[8]
Sender Embedding Size	[128]
Sender Meaning LSTM Hidden Size	[128]
Sender Temporal LSTM Hidden Size	[128]
Sender Message LSTM Hidden Size	[128]
Receiver LSTM+Linear Hidden Size	[128]
Gumbel-Softmax Temperature	[1.0]

Table 4: Compute Resources

Resource	Quantity
CPU Cores (Intel(R) Xeon(R) Silver 4216 \times 2)	20
GPUs (NVIDIA Quadro RTX8000)	1
Wall Time	28hrs

Appendix B. Datasets Details

In Figure 6, we analyse our datasets, using the parameters as specified in Appendix A, for the number of repetitions that occur. When the temporal dataset repetition chance is set to 50%, the datasets, predictably, oscillate around 50% of repeating targets. Generating the targets randomly yields a miniscule fraction of repetitions of less than 1%, as we can see in Figure 6, for the Classic and Hard referential games.

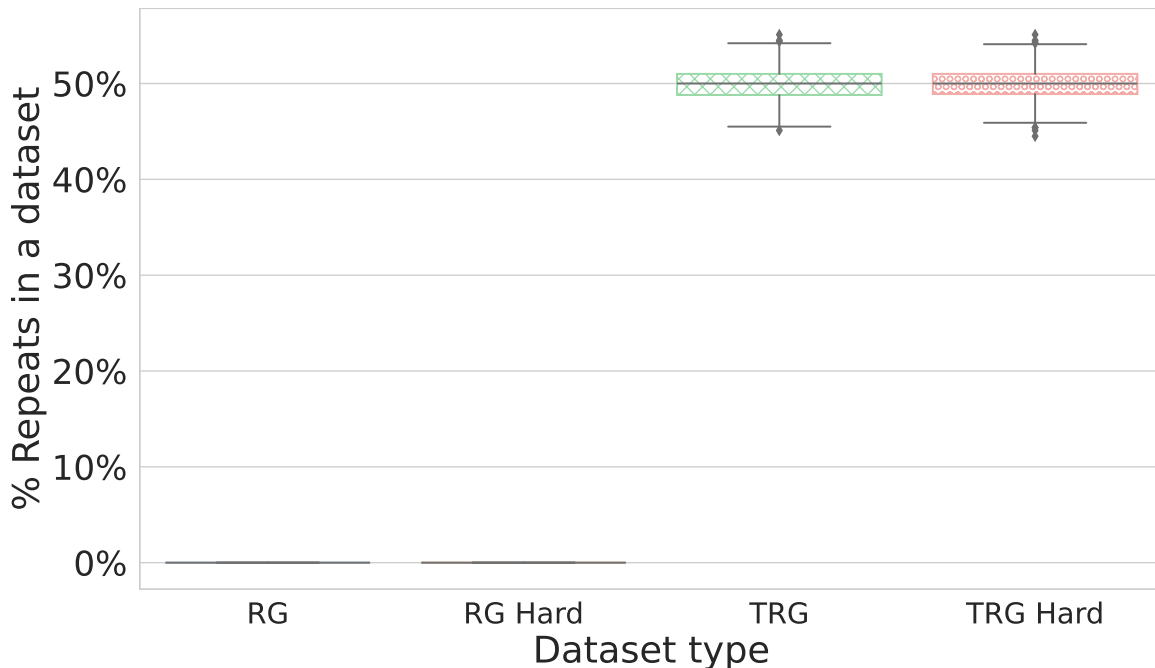


Figure 6: Number of target repetitions per dataset. Regular referential games datasets very rarely encounter target repetitions. This data is an average over 1000 seeds per environment.

B.1 Test Environments

Both Always Same and Never Same environments act as sanity checks for our results.

We provide example inputs and outputs for both environments in Table 5 and Table 6. We use single-attribute objects and messages for clarity.

For the Always Same environment, in the case of the agent using temporal references, we may also see other messages instead of the message m_4 , as we have observed that there are more than one message used as previously. We always expect to see at most 90% of usage as previously for this environment, unless the agents learn temporal referencing strategies, when we would expect the usage to reach 100%.

For the Never Same environment, we expect to see no temporal references being identified. Any identification of temporal references in the Never Same environment would indicate an issue with our metric.

Table 5: Example Inputs and Outputs for Always Same.

Environment	Always Same
Input	$[x, x, x, y, y, y, z, z, z]$
Temporal Referencing	$[m_1, m_4, m_4, m_2, m_4, m_4, m_3, m_4, m_4]$
No Temporal Referencing	$[m_1, m_2, m_3, m_4, m_5, m_6, m_7, m_8]$

Table 6: Example Inputs and Outputs for Never Same.

Environment	Never Same
Input	$[x, y, z, a, b, c, d, e]$
Temporal Referencing	$[m_1, m_1, m_1, m_2, m_2, m_2, m_3, m_3, m_3]$
No Temporal Referencing	$[m_1, m_2, m_3, m_4, m_5, m_6, m_7, m_8]$

Appendix C. Architecture Overview

In Figure 7, we present an overview of our whole experimental setup. We can see the sender and receiver architectures, together with their inputs, as described in Section 3. We also show our loss calculations.

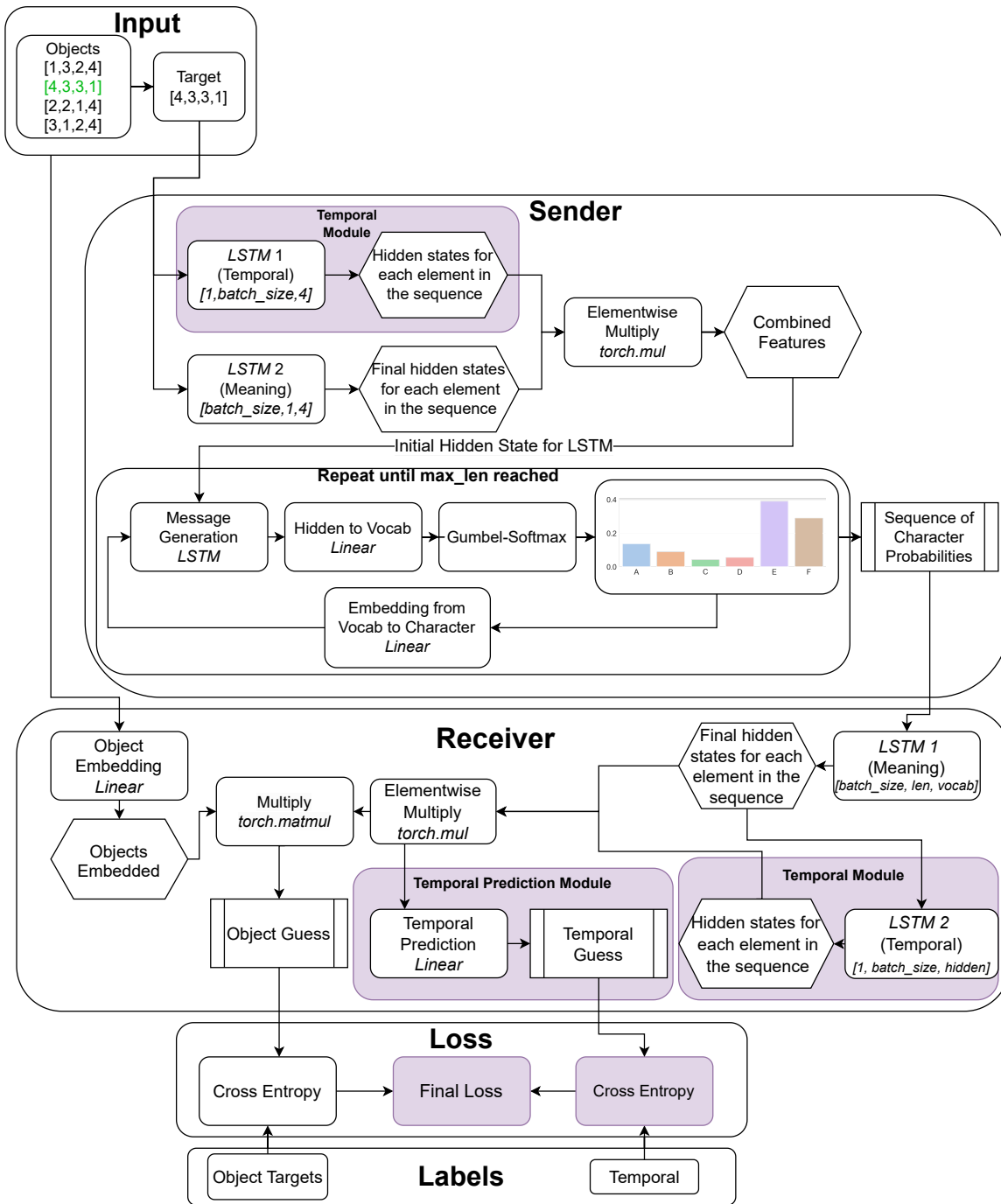
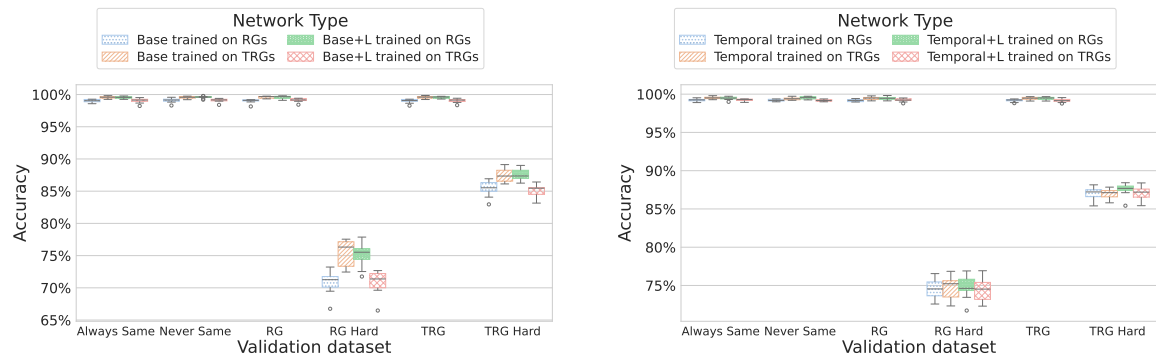


Figure 7: Full overview of our Temporal Referential Games setup. Together with the sender and receiver we have described in Section 3, we also include the working of the loss.

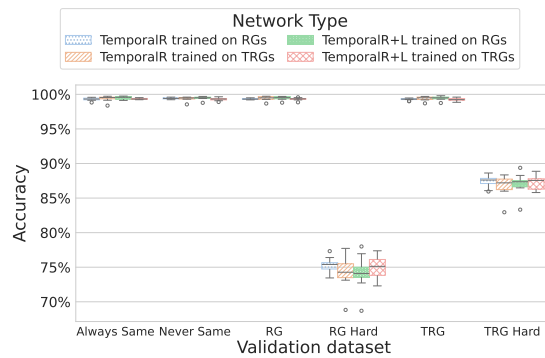
Appendix D. Accuracy Distributions

The accuracy distributions for all agent types across all evaluation environments are shown in Figures 8a to 8c. All agents converge to very similar levels of accuracy.



(a) The evaluation accuracy for the *Base* agents across all environments.

(b) The evaluation accuracy for the *Temporal* agents across all environments.

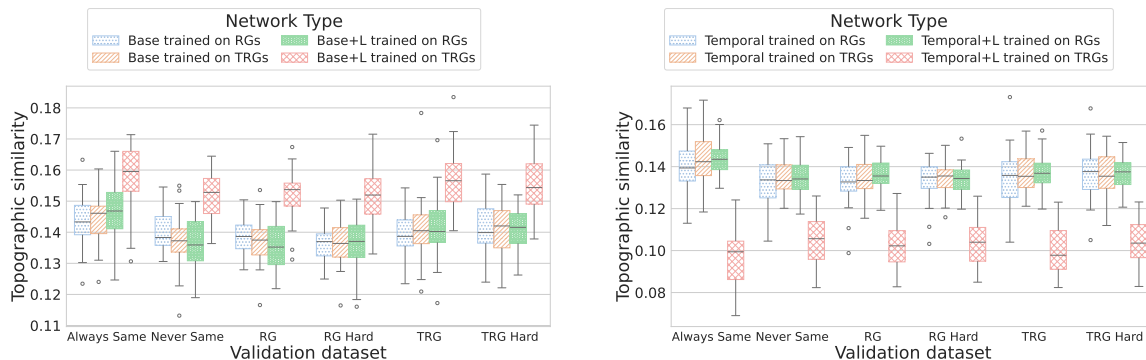


(c) The evaluation accuracy for the *TemporalR* agents across all environments.

Figure 8: Accuracies for each network variant on all evaluation environments.

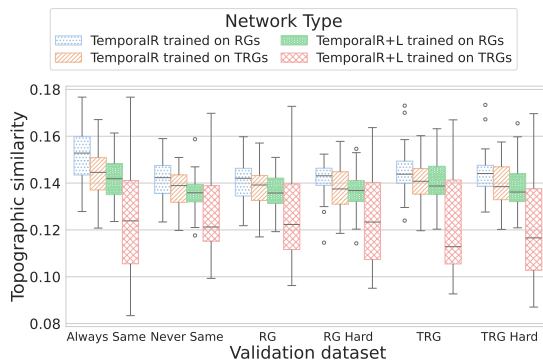
Appendix E. Topographic Similarity Distributions

The topographic similarity distributions for all agent types across all evaluation environments are shown in Figures 9a to 9c. All agents converge to very similar values of topographic similarity.



(a) The topographic similarity scores for the *Base* agents across all environments.

(b) The topographic similarity scores for the *Temporal* agents across all environments.



(c) The topographic similarity scores for the *TemporalR* agents across all environments.

Figure 9: Topographic similarity scores for each network variant on all evaluation environments.

Appendix F. Supplementary Material

F.1 Temporality analysis for previous horizon from $h_v = 1$ to $h_v = 8$

In Table 7, we can see the absolute percentages of networks which develop temporal references.

The full plots for all metrics are shown for previous horizon from $h_v = 1$ to $h_v = 8$. The M_{\ominus^h} metric values for the Base, Temporal, TemporalR and Attention agents are available in Figures 10 to 13. The correctness of the messages used as the \ominus^h operator for each agent type is available in Figures 14 to 16. No Base networks feature in the plots, as they do not develop temporal references, and so there are no messages to measure the correctness of.

Table 7: Emergence of temporal references for a given horizon.

Network Type	$h_v = 1$	$h_v = 2$	$h_v = 3$	$h_v = 4$	$h_v = 5$	$h_v = 6$	$h_v = 7$	$h_v = 8$
Base	0%	0%	0%	0%	0%	0%	0%	0%
Base+L	0%	0%	0%	0%	0%	0%	0%	0%
Temporal	100%	100%	100%	100%	100%	100%	100%	100%
Temporal+L	100%	100%	100%	100%	100%	100%	100%	100%
TemporalR	98.89%	100%	100%	99.44%	97.22%	100%	99.44%	97.78%
TemporalR+L	99.44%	100%	99.44%	98.89%	98.89%	99.44%	99.44%	98.89%
Attention	99.63%	100%	100%	100%	100%	99.81%	100%	100%
Attention+L	99.81%	100%	100%	100%	100%	100%	100%	100%



Figure 10: The M_{Θ^h} metric values per message for the *Base* agents, for all environments.

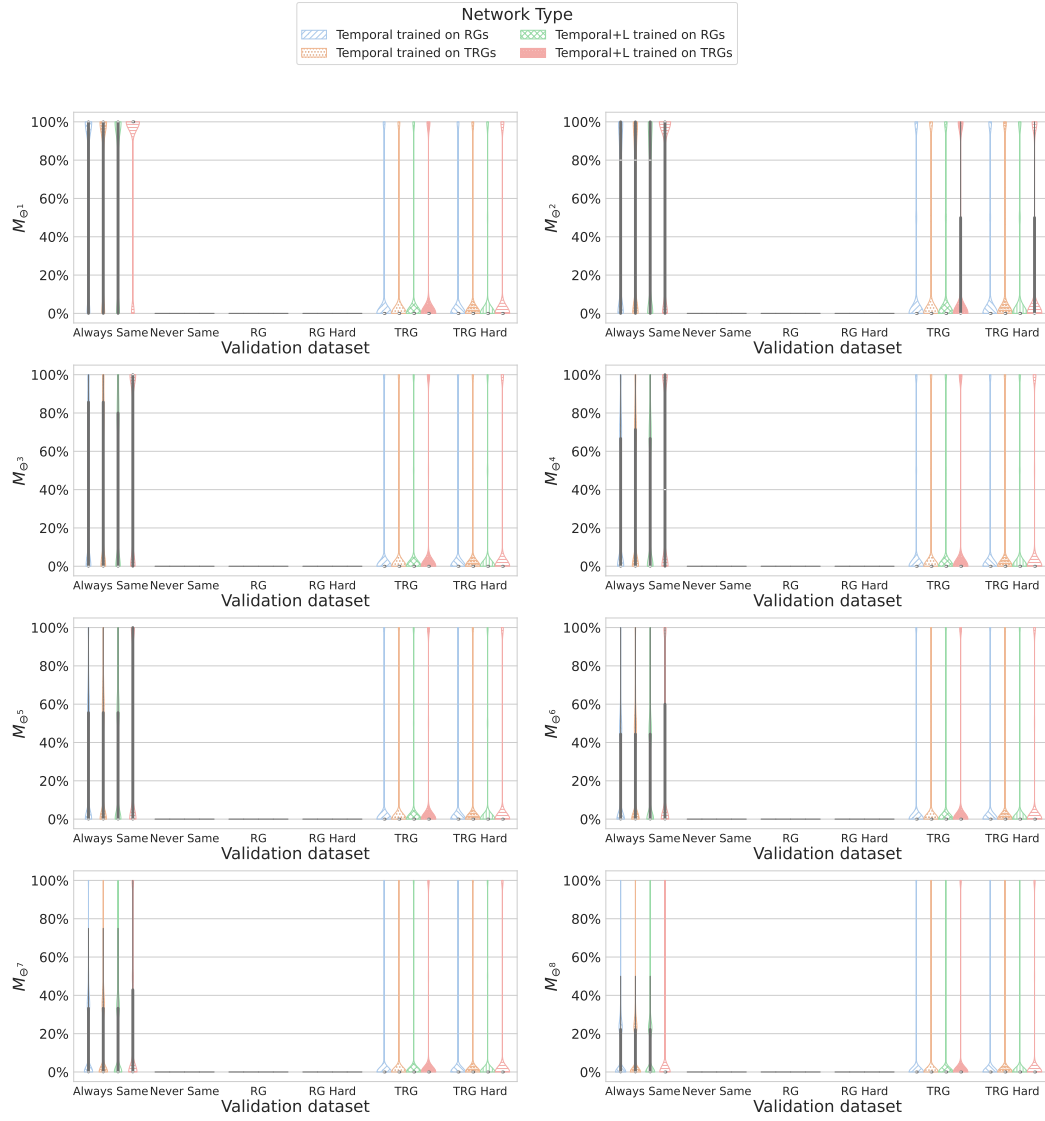


Figure 11: The M_{Θ^h} metric values per message for the *Temporal* agents, for all environments.



Figure 12: The M_{Θ^h} metric values per message for the *TemporalR* agents, for all environments.



Figure 13: The M_{Θ^h} metric values per message for the *Attention* agents, for all environments.

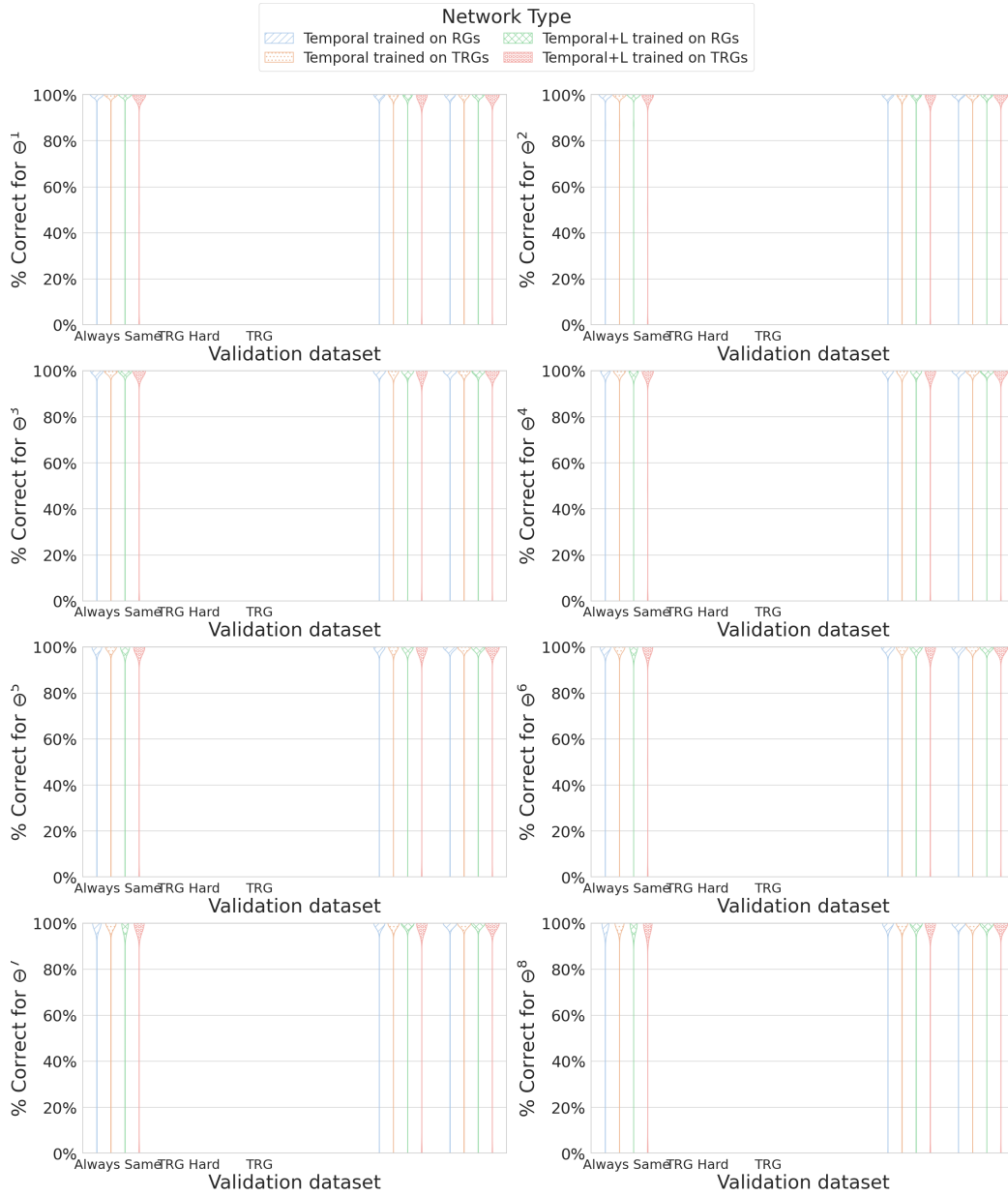


Figure 14: Correctness of messages used as the Θ^h operator for the *Temporal* agents.

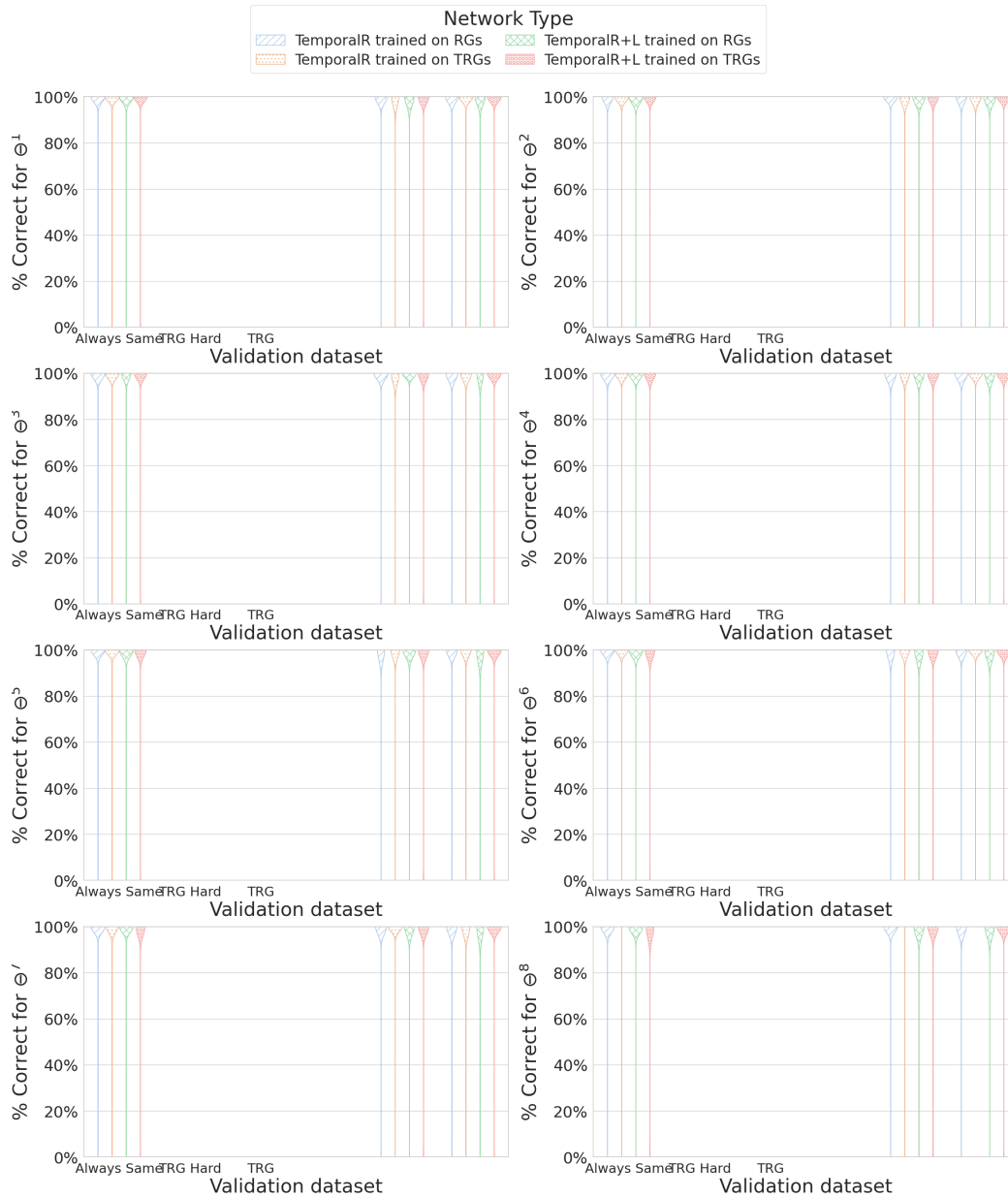


Figure 15: Correctness of messages used as the Θ^h operator for the *TemporalR* agents.

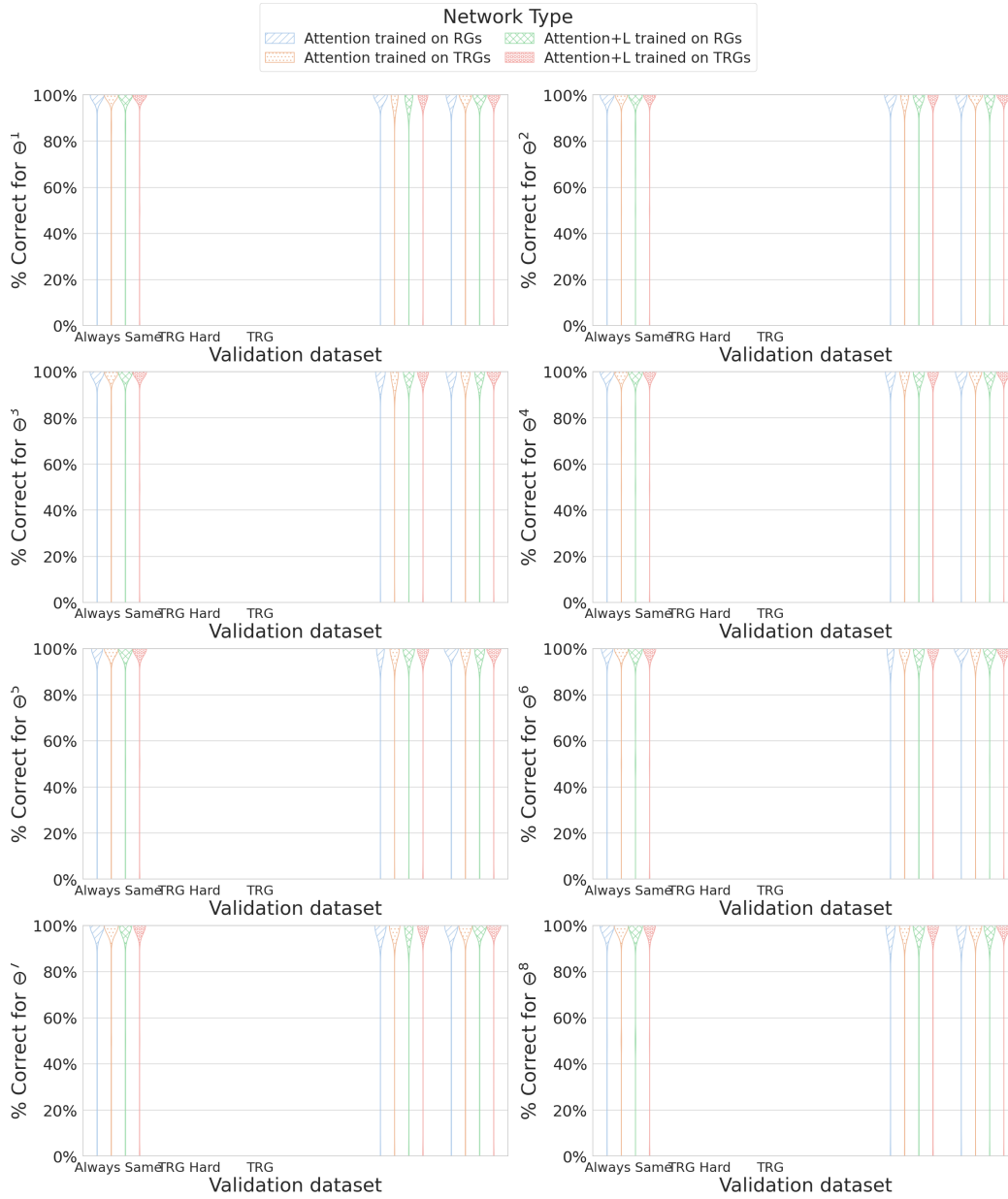


Figure 16: Correctness of messages used as the Θ^h operator for the *Attention* agents.

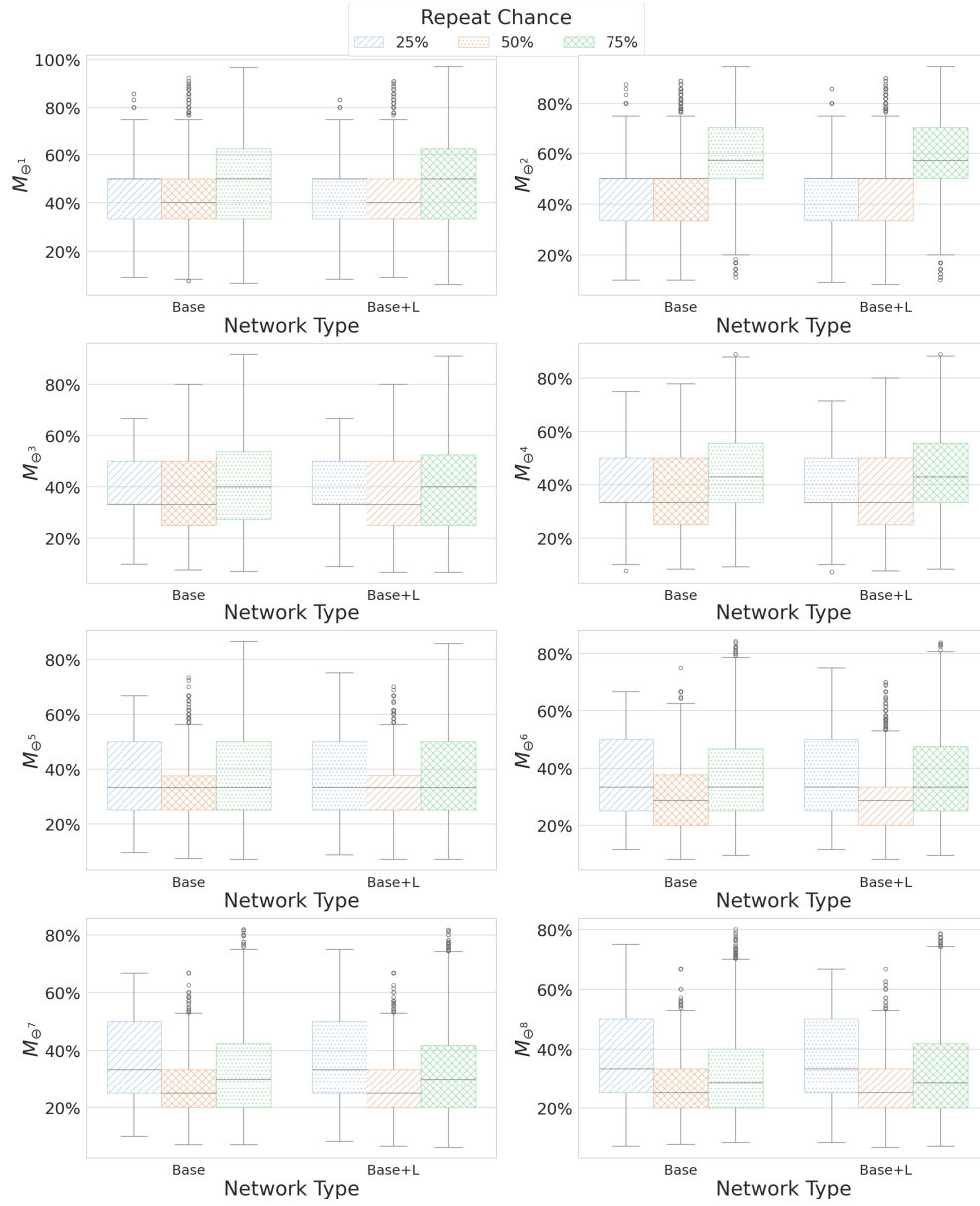


Figure 17: The M_{Θ^h} value when varying the loss and the chance of repetition for the *Base* agents.

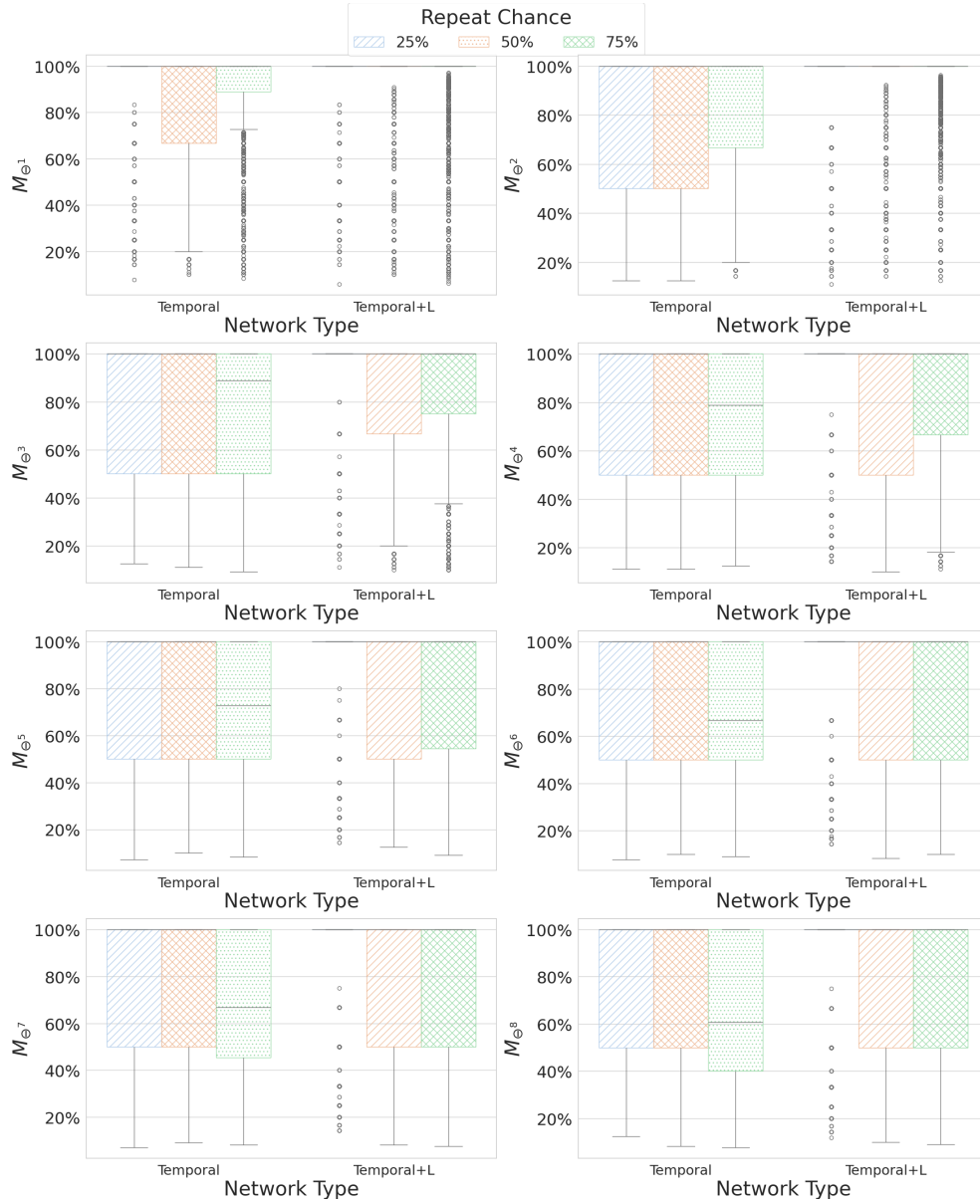


Figure 18: The M_{Θ^h} value when varying the loss and the chance of repetition for the *Temporal* agents.

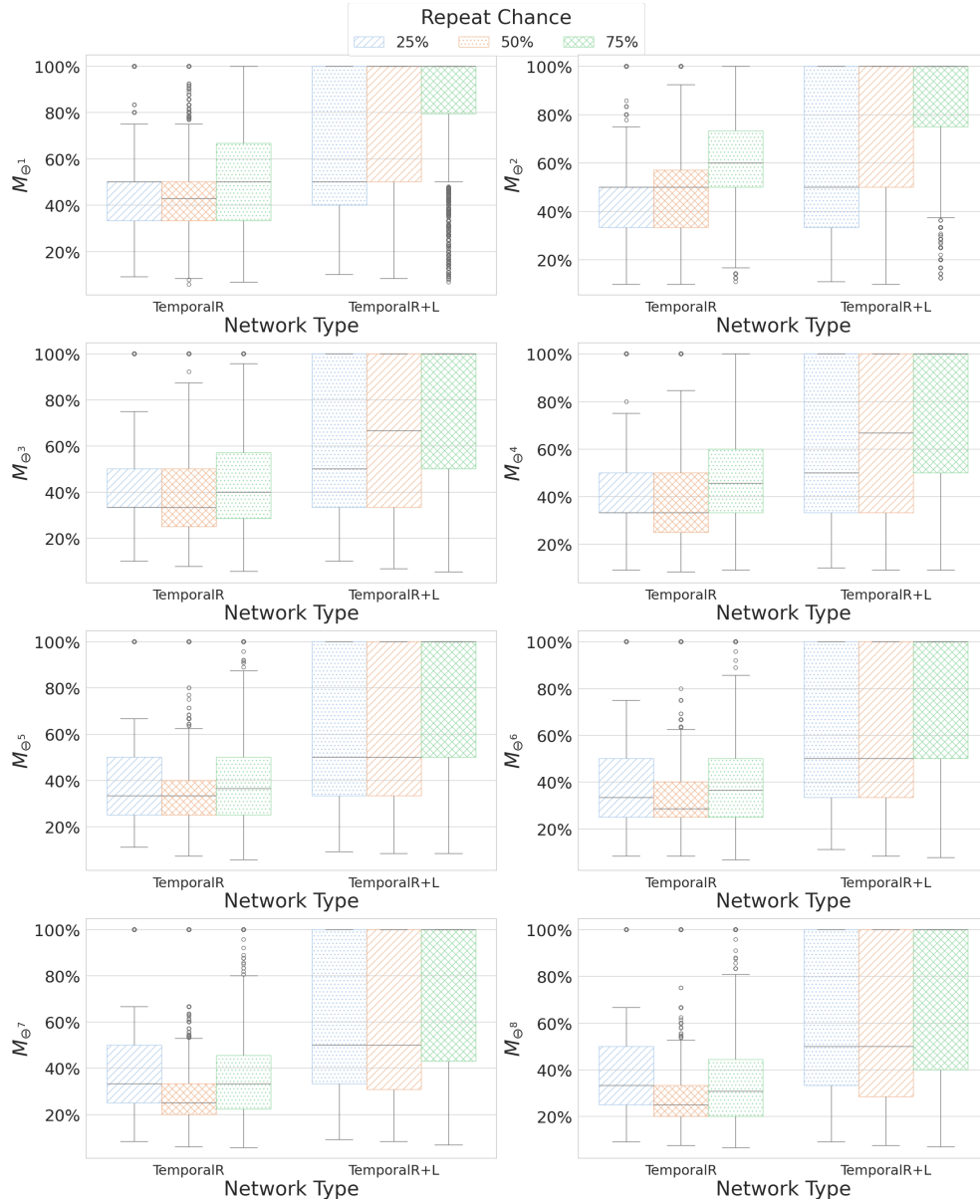


Figure 19: The M_{Θ^h} value when varying the loss and the chance of repetition for the *TemporalR* agents.

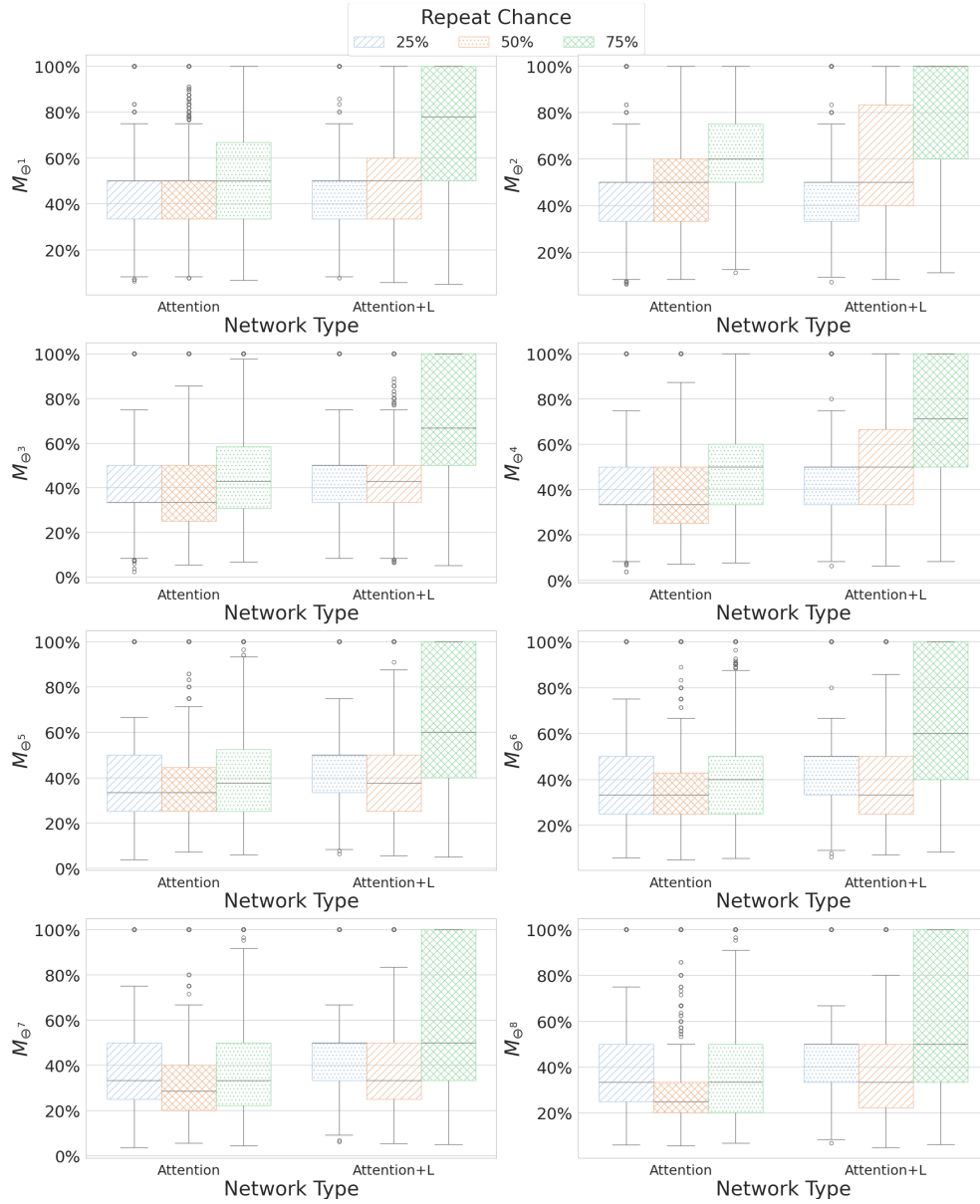


Figure 20: The M_{Θ^h} value when varying the loss and the chance of repetition for the *Attention* agents.

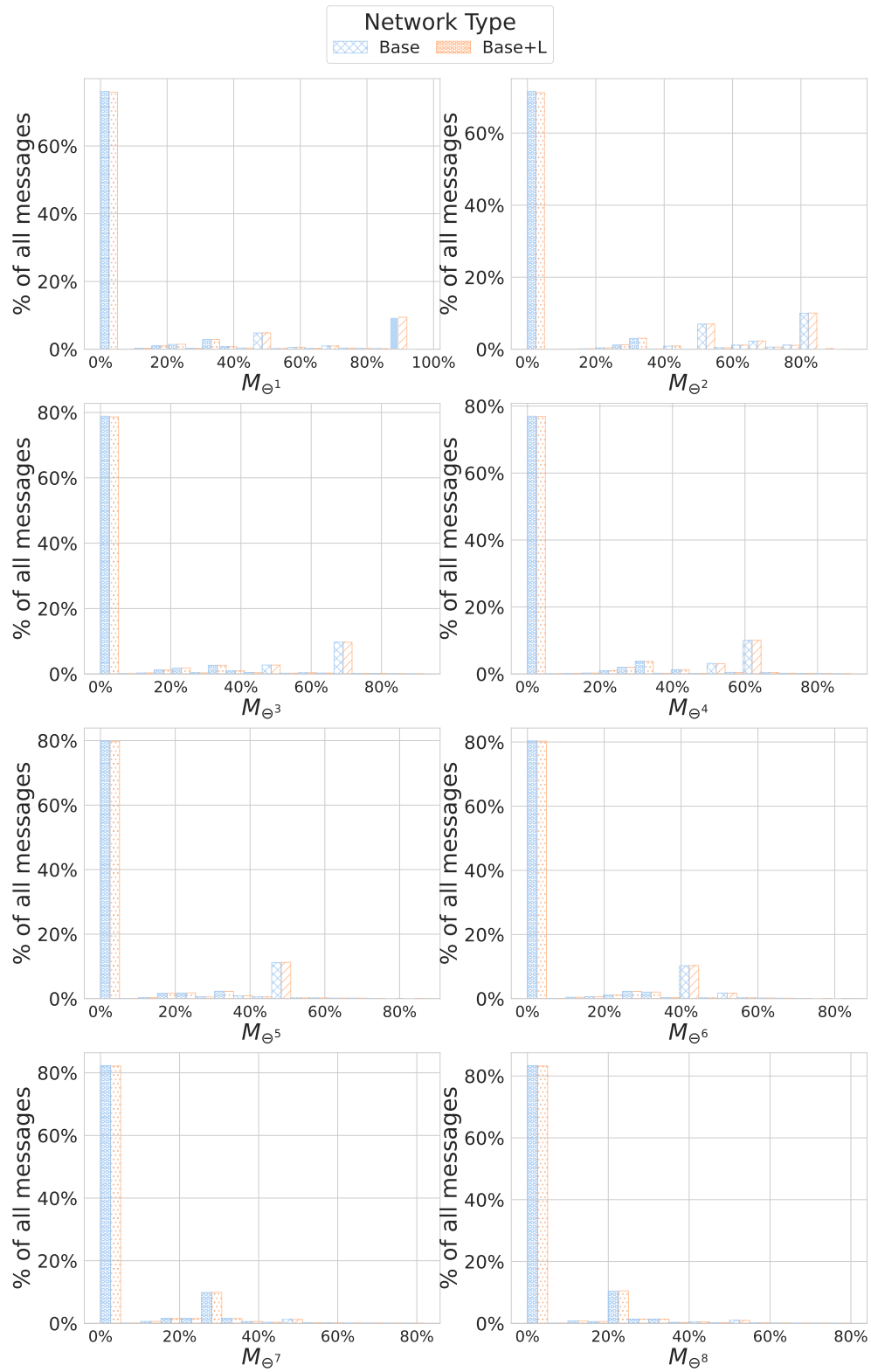


Figure 21: Usage of messages compared to their M_{Θ^h} value for the *Base* agents.

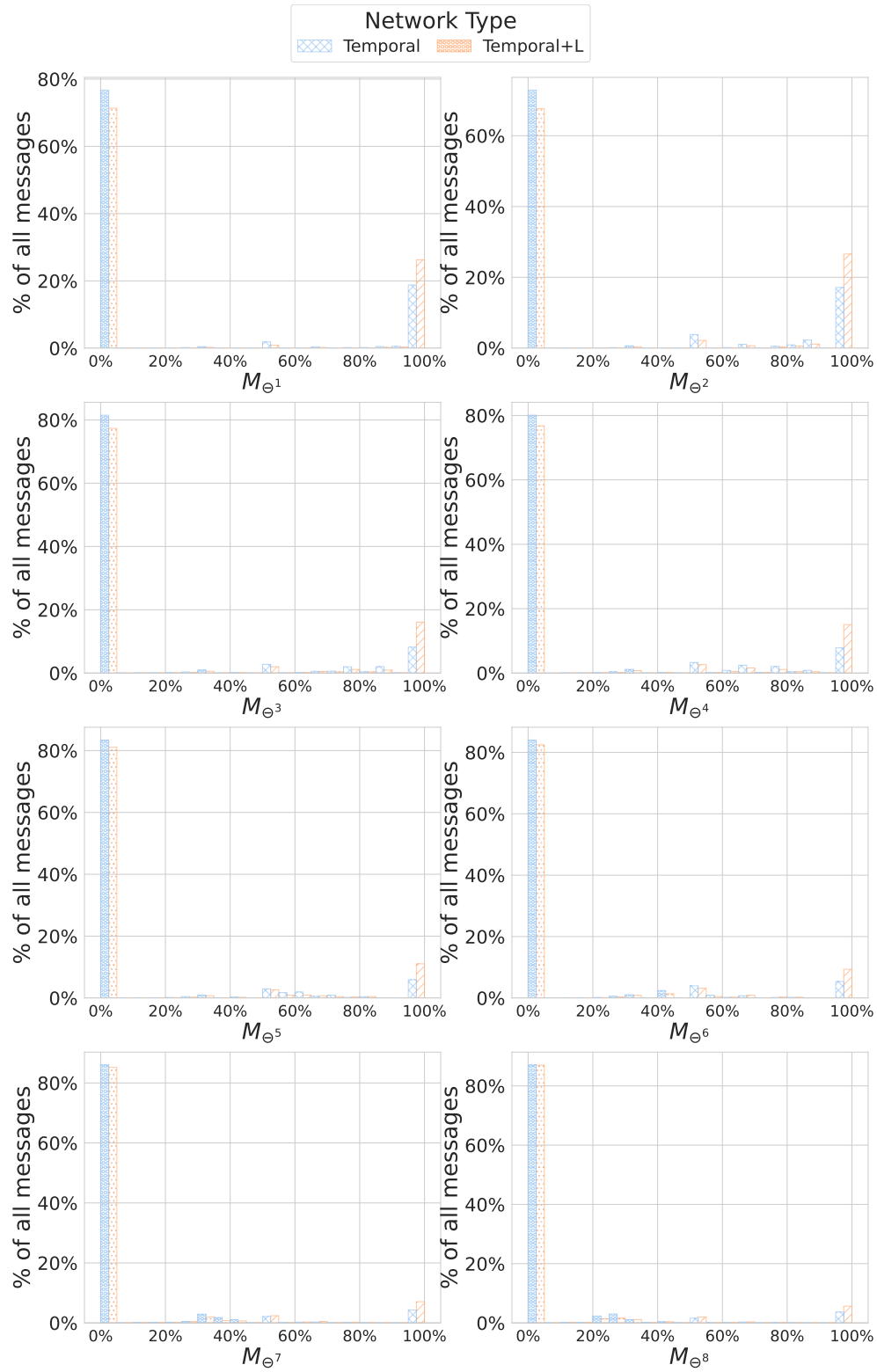


Figure 22: Usage of messages compared to their M_{Θ^h} value for the *Temporal* agents.

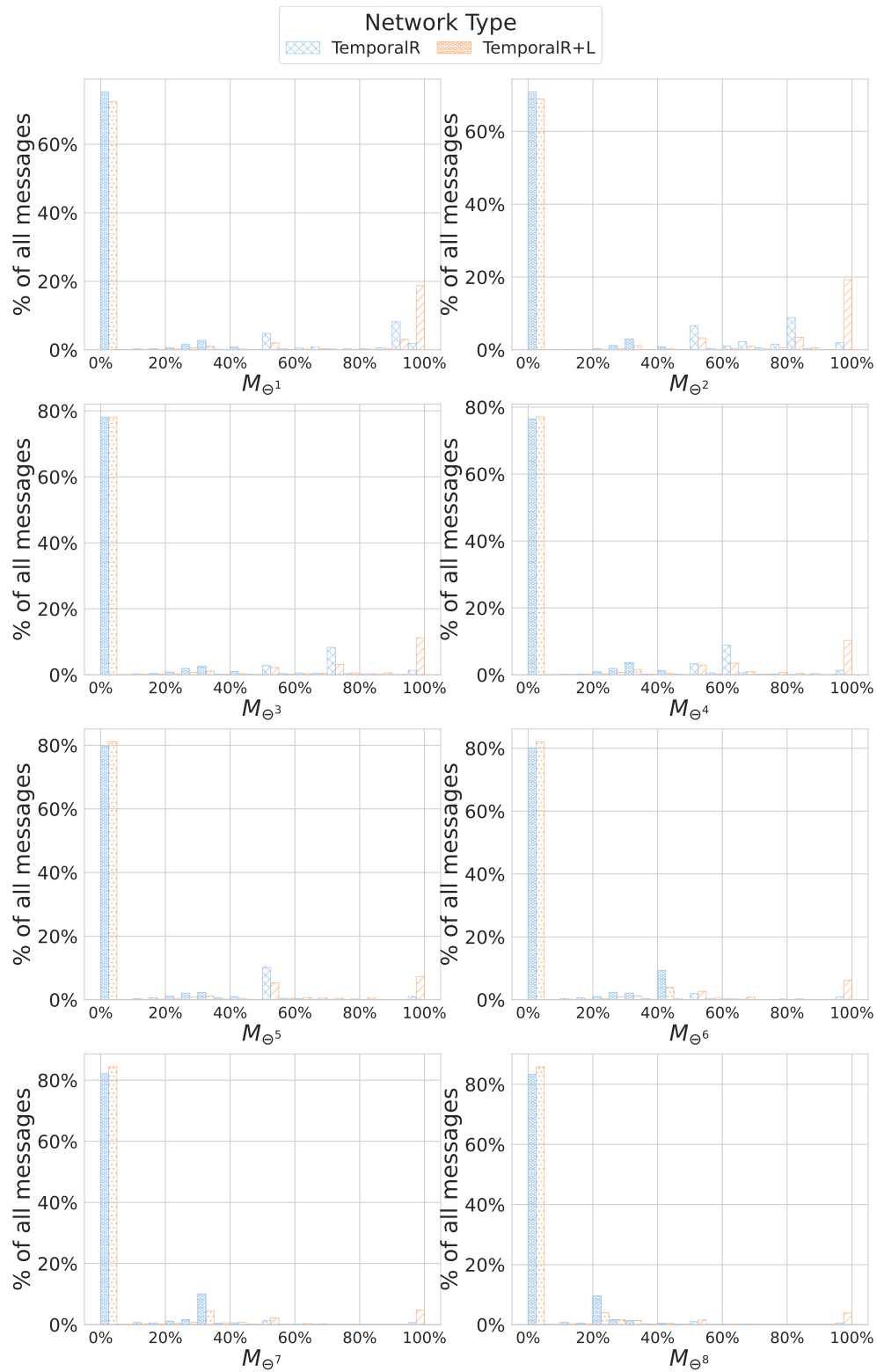
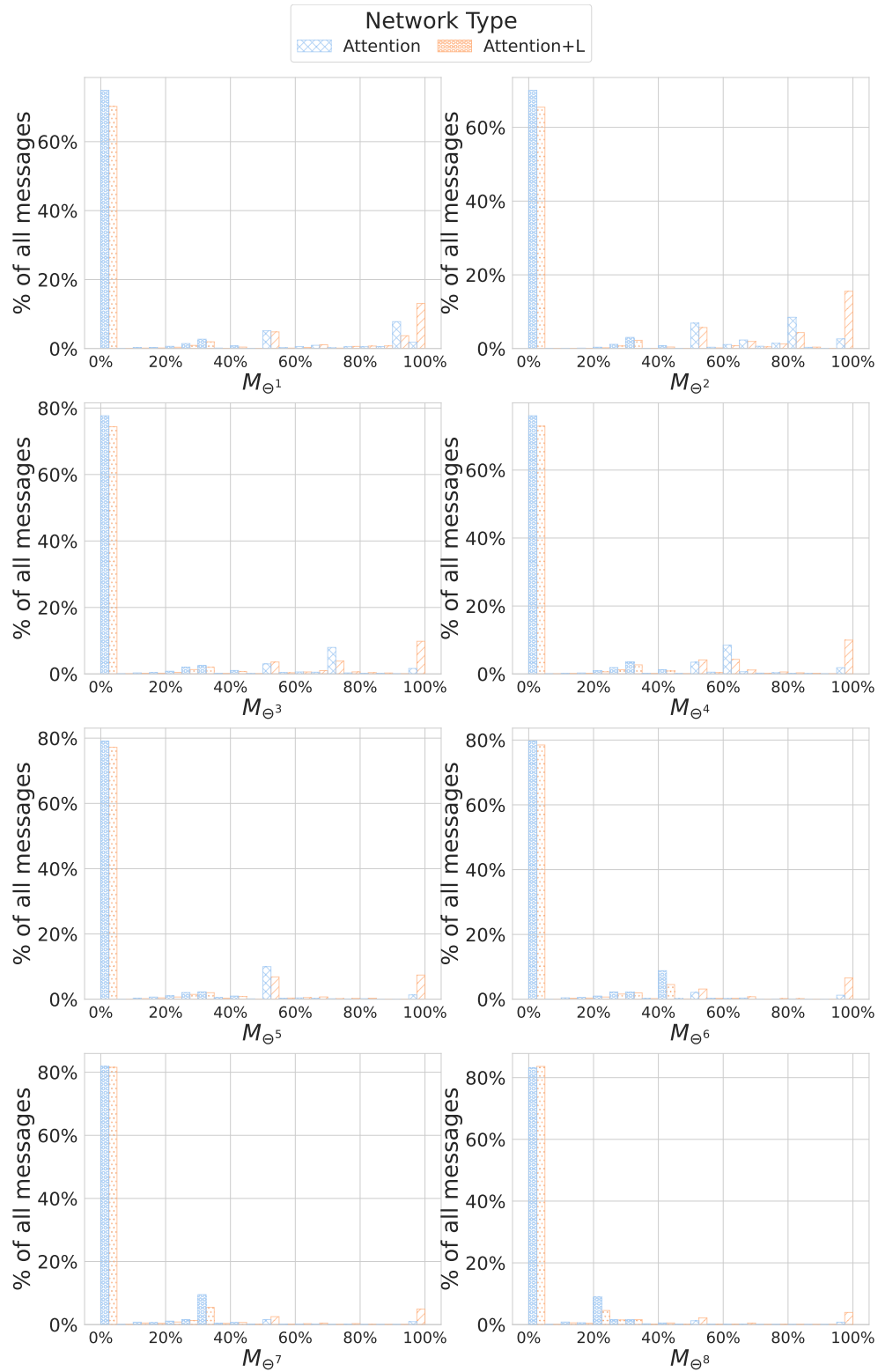


Figure 23: Usage of messages compared to their M_{Θ^h} value for the *TemporalR* agents.

Figure 24: Usage of messages compared to their M_{Θ^h} value for the *Attention* agents.

F.2 Analysis within Network Types

In this section, the detailed values of all statistical significance tests are provided.

F.2.1 NORMALITY TESTS

Network Type	Training Env	Always Same	Never Same	RG	RG Hard	TRG	TRG Hard
Base	RG	0.01	0.01	0.01	0.02	0.01	0.02
	TRG	0.39	0.04	0.02	0.01	0.01	0.01
Base+L	RG	0.01	0.01	0.01	0.73	0.08	0.01
	TRG	0.18	0.25	0.98	0.42	0.24	0.01
Temporal	RG	0.11	0.65	0.22	0.86	0.69	0.01
	TRG	0.01	0.01	0.01	0.02	0.01	0.01
Temporal+L	RG	0.02	0.07	0.08	0.46	0.48	0.01
	TRG	0.03	0.78	0.82	0.80	0.60	0.01
TemporalR	RG	0.09	0.68	0.27	0.04	0.16	0.01
	TRG	0.02	0.01	0.02	0.05	0.25	0.01
TemporalR+L	RG	0.03	0.01	0.37	0.28	0.63	0.01
	TRG	0.06	0.10	0.21	0.30	0.34	0.01
Attention	RG	0.42	0.18	0.50	0.63	0.10	0.20
	TRG	0.01	0.01	0.01	0.01	0.01	0.01
Attention+L	RG	0.11	0.73	0.17	0.61	0.98	0.01
	TRG	0.16	0.06	0.27	0.93	0.94	0.01

Table 8: p values for the normality test on the accuracy scores.

Network Type	Training Env	Always Same	Never Same	RG	RG Hard	TRG	TRG Hard
Base	RG	NaN	N/A	NaN	NaN	0	0
	TRG	NaN	N/A	NaN	NaN	0	0
Base+L	RG	NaN	N/A	NaN	NaN	0	0
	TRG	NaN	N/A	NaN	NaN	0	0
Temporal	RG	0	N/A	NaN	NaN	0	0
	TRG	0	N/A	NaN	NaN	0	0
Temporal+L	RG	0	N/A	NaN	NaN	0	0
	TRG	0	N/A	NaN	NaN	0	0
TemporalR	RG	0	N/A	NaN	NaN	0	0
	TRG	0	N/A	NaN	NaN	0	0
TemporalR+L	RG	0	N/A	NaN	NaN	0	0
	TRG	0	N/A	NaN	NaN	0	0
Attention	RG	0	N/A	NaN	NaN	0	0
	TRG	0	N/A	NaN	NaN	0	0
Attention+L	RG	0	N/A	NaN	NaN	0	0
	TRG	0	N/A	NaN	NaN	0	0

Table 9: p values for the normality test on the M_{\ominus^n} scores.

Network Type	Training Env	TopSim	Posdis	Bosdis
Base	RG	0.01	0.01	0.75
	TRG	0.44	0.01	0.90
Base+L	RG	0.31	0.02	0.05
	TRG	0.91	0.01	0.01
Temporal	RG	0.11	0.01	0.02
	TRG	0.38	0.02	0.01
Temporal+L	RG	0.05	0.01	0.14
	TRG	0.38	0.01	0.80
TemporalR	RG	0.97	0.10	0.32
	TRG	0.34	0.08	0.52
TemporalR+L	RG	0.02	0.01	0.83
	TRG	0.01	0.02	0.01
Attention	RG	0.33	0.01	0.15
	TRG	0.36	0.01	0.02
Attention+L	RG	0.01	0.01	0.01
	TRG	0.01	0.01	0.38

Table 10: p values for the normality test on the compositionality scores.

F.2.2 ACCURACY KRUSKAL-WALLIS H-TEST P-VALUES WITHIN NETWORK TYPES

	Always Same	Never Same	RG	RG Hard	TRG	TRG Hard
Base	0	0	0	0	0	0.060617
Temporal	0	0	0	0	0	0.000197
TemporalR	0	0	0	0	0	0.004879
Attention	0.000010	0.000021	0.000094	0	0.000126	0.158000

Table 11: p values of the Kruskal-Wallis H-test for the accuracy scores within a given network type.

F.2.3 ACCURACY POST-HOC CONOVER ANALYSIS WITHIN NETWORK TYPES

	Base+L RG	Base RG	Base+L TRG	Base RG
Base+L RG	1	0.433259	0	0.498274
Base RG	0.433259	1	0	0.171310
Base+L TRG	0	0	1	0
Base RG	0.498274	0.171310	0	1

Table 12: p values of the post-hoc Conover test for the accuracy scores on the Always Same environment.

	Base+L RG	Base RG	Base+L TRG	Base RG
Base+L RG	1	0.433899	0	0.582182
Base RG	0.433899	1	0	0.226648
Base+L TRG	0	0	1	0
Base RG	0.582182	0.226648	0	1

Table 13: p values of the post-hoc Conover test for the accuracy scores on the Never Same environment.

	Base+L RG	Base RG	Base+L TRG	Base RG
Base+L RG	1	0.149439	0	0.668939
Base RG	0.149439	1	0	0.083620
Base+L TRG	0	0	1	0
Base RG	0.668939	0.083620	0	1

Table 14: p values of the post-hoc Conover test for the accuracy scores on the RG environment.

	Base+L RG	Base RG	Base+L TRG	Base RG
Base+L RG	1	0.346337	0	0.346337
Base RG	0.346337	1	0	0.040696
Base+L TRG	0	0	1	0
Base RG	0.346337	0.040696	0	1

Table 15: p values of the post-hoc Conover test for the accuracy scores on the RG Hard environment.

	Base+L RG	Base RG	Base+L TRG	Base RG
Base+L RG	1	0.185363	0	0.185363
Base RG	0.185363	1	0	0.005564
Base+L TRG	0	0	1	0
Base RG	0.185363	0.005564	0	1

Table 16: p values of the post-hoc Conover test for the accuracy scores on the TRG environment.

	Base+L RG	Base RG	Base+L TRG	Base RG
Base+L RG	1	1	0.175554	1
Base RG	1	1	0.087409	1
Base+L TRG	0.175554	0.087409	1	0.175554
Base RG	1	1	0.175554	1

Table 17: p values of the post-hoc Conover test for the accuracy scores on the TRG Hard environment.

	Temporal+L RG	Temporal RG	Temporal+L TRG	Temporal RG
Temporal+L RG	1	1	0	1
Temporal RG	1	1	0	1
Temporal+L TRG	0	0	1	0
Temporal RG	1	1	0	1

Table 18: p values of the post-hoc Conover test for the accuracy scores on the Always Same environment.

	Temporal+L RG	Temporal RG	Temporal+L TRG	Temporal RG
Temporal+L RG	1	0.876314	0	0.114027
Temporal RG	0.876314	1	0	0.114027
Temporal+L TRG	0	0	1	0
Temporal RG	0.114027	0.114027	0	1

Table 19: p values of the post-hoc Conover test for the accuracy scores on the Never Same environment.

	Temporal+L RG	Temporal RG	Temporal+L TRG	Temporal RG
Temporal+L RG	1	0.384963	0	0.635388
Temporal RG	0.384963	1	0	0.229984
Temporal+L TRG	0	0	1	0
Temporal RG	0.635388	0.229984	0	1

Table 20: p values of the post-hoc Conover test for the accuracy scores on the RG environment.

	Temporal+L RG	Temporal RG	Temporal+L TRG	Temporal RG
Temporal+L RG	1	0.056940	0	0.000033
Temporal RG	0.056940	1	0	0.017182
Temporal+L TRG	0	0	1	0
Temporal RG	0.000033	0.017182	0	1

Table 21: p values of the post-hoc Conover test for the accuracy scores on the RG Hard environment.

	Temporal+L RG	Temporal RG	Temporal+L TRG	Temporal RG
Temporal+L RG	1	1	0	1
Temporal RG	1	1	0	1
Temporal+L TRG	0	0	1	0
Temporal RG	1	1	0	1

Table 22: p values of the post-hoc Conover test for the accuracy scores on the TRG environment.

	Temporal+L RG	Temporal RG	Temporal+L TRG	Temporal RG
Temporal+L RG	1	0.993318	0.000135	0.691546
Temporal RG	0.993318	1	0.001456	0.993318
Temporal+L TRG	0.000135	0.001456	1	0.006804
Temporal RG	0.691546	0.993318	0.006804	1

Table 23: p values of the post-hoc Conover test for the accuracy scores on the TRG Hard environment.

	TemporalR+L RG	TemporalR RG	TemporalR+L TRG	TemporalR RG
TemporalR+L RG	1	0.442920	0	0.442920
TemporalR RG	0.442920	1	0	0.071027
TemporalR+L TRG	0	0	1	0
TemporalR RG	0.442920	0.071027	0	1

Table 24: p values of the post-hoc Conover test for the accuracy scores on the Always Same environment.

	TemporalR+L RG	TemporalR RG	TemporalR+L TRG	TemporalR RG
TemporalR+L RG	1	0.224358	0	0.084598
TemporalR RG	0.224358	1	0	0.004183
TemporalR+L TRG	0	0	1	0
TemporalR RG	0.084598	0.004183	0	1

Table 25: p values of the post-hoc Conover test for the accuracy scores on the Never Same environment.

	TemporalR+L RG	TemporalR RG	TemporalR+L TRG	TemporalR RG
TemporalR+L RG	1	0.009688	0	0.512991
TemporalR RG	0.009688	1	0	0.040779
TemporalR+L TRG	0	0	1	0
TemporalR RG	0.512991	0.040779	0	1

Table 26: p values of the post-hoc Conover test for the accuracy scores on the RG environment.

	TemporalR+L RG	TemporalR RG	TemporalR+L TRG	TemporalR RG
TemporalR+L RG	1	0.589040	0	0.871791
TemporalR RG	0.589040	1	0	0.589040
TemporalR+L TRG	0	0	1	0
TemporalR RG	0.871791	0.589040	0	1

Table 27: p values of the post-hoc Conover test for the accuracy scores on the RG Hard environment.

	TemporalR+L RG	TemporalR RG	TemporalR+L TRG	TemporalR RG
TemporalR+L RG	1	0.015392	0	0.481321
TemporalR RG	0.015392	1	0	0.002605
TemporalR+L TRG	0	0	1	0
TemporalR RG	0.481321	0.002605	0	1

Table 28: p values of the post-hoc Conover test for the accuracy scores on the TRG environment.

	TemporalR+L RG	TemporalR RG	TemporalR+L TRG	TemporalR RG
TemporalR+L RG	1	1	0.011330	1
TemporalR RG	1	1	0.012271	1
TemporalR+L TRG	0.011330	0.012271	1	0.018447
TemporalR RG	1	1	0.018447	1

Table 29: p values of the post-hoc Conover test for the accuracy scores on the TRG Hard environment.

	Attention+L RG	Attention RG	Attention+L TRG	Attention RG
Attention+L RG	1	1	0.000021	1
Attention RG	1	1	0.000378	1
Attention+L TRG	0.000021	0.000378	1	0.000024
Attention RG	1	1	0.000024	1

Table 30: p values of the post-hoc Conover test for the accuracy scores on the Always Same environment.

	Attention+L RG	Attention RG	Attention+L TRG	Attention RG
Attention+L RG	1	1	0.000021	1
Attention RG	1	1	0.000446	1
Attention+L TRG	0.000021	0.000446	1	0.000151
Attention RG	1	1	0.000151	1

Table 31: p values of the post-hoc Conover test for the accuracy scores on the Never Same environment.

	Attention+L RG	Attention RG	Attention+L TRG	Attention RG
Attention+L RG	1	1	0.000132	1
Attention RG	1	1	0.001192	1
Attention+L TRG	0.000132	0.001192	1	0.000509
Attention RG	1	1	0.000509	1

Table 32: p values of the post-hoc Conover test for the accuracy scores on the RG environment.

	Attention+L RG	Attention RG	Attention+L TRG	Attention RG
Attention+L RG	1	0.922225	0	0.922225
Attention RG	0.922225	1	0	0.922225
Attention+L TRG	0	0	1	0
Attention RG	0.922225	0.922225	0	1

Table 33: p values of the post-hoc Conover test for the accuracy scores on the RG Hard environment.

	Attention+L RG	Attention RG	Attention+L TRG	Attention RG
Attention+L RG	1	1	0.000467	1
Attention RG	1	1	0.000534	1
Attention+L TRG	0.000467	0.000534	1	0.000534
Attention RG	1	1	0.000534	1

Table 34: p values of the post-hoc Conover test for the accuracy scores on the TRG environment.

	Attention+L RG	Attention RG	Attention+L TRG	Attention RG
Attention+L RG	1	1	0.336244	1
Attention RG	1	1	0.336244	1
Attention+L TRG	0.336244	0.336244	1	0.321269
Attention RG	1	1	0.321269	1

Table 35: p values of the post-hoc Conover test for the accuracy scores on the TRG Hard environment.

F.2.4 TOPOGRAPHIC SIMILARITY POST-HOC CONOVER ANALYSIS WITHIN NETWORK TYPES

	Base+L RG	Base RG	Base+L TRG	Base RG
Base+L RG	1	1	0	1
Base RG	1	1	0	1
Base+L TRG	0	0	1	0
Base RG	1	1	0	1

Table 36: p values of the post-hoc Conover test for the topographic similarity scores.

	Temporal+L RG	Temporal RG	Temporal+L TRG	Temporal RG
Temporal+L RG	1	0.271644	0	0.075936
Temporal RG	0.271644	1	0	0.454652
Temporal+L TRG	0	0	1	0
Temporal RG	0.075936	0.454652	0	1

Table 37: p values of the post-hoc Conover test for the topographic similarity scores.

	TemporalR+L RG	TemporalR RG	TemporalR+L TRG	TemporalR RG
TemporalR+L RG	1	0.000081	0	0
TemporalR RG	0.000081	1	0	0.131500
TemporalR+L TRG	0	0	1	0
TemporalR RG	0	0.131500	0	1

Table 38: p values of the post-hoc Conover test for the topographic similarity scores.

F.2.5 POSITIONAL DISENTANGLEMENT POST-HOC CONOVER ANALYSIS WITHIN NETWORK TYPES

	Attention+L RG	Attention RG	Attention+L TRG	Attention RG
Attention+L RG	1	0.944386	0	0.078594
Attention RG	0.944386	1	0	0.078594
Attention+L TRG	0	0	1	0
Attention RG	0.078594	0.078594	0	1

Table 39: p values of the post-hoc Conover test for the topographic similarity scores.

	Base+L RG	Base RG	Base+L TRG	Base RG
Base+L RG	1	1	0	0.967127
Base RG	1	1	0	1
Base+L TRG	0	0	1	0
Base RG	0.967127	1	0	1

Table 40: p values of the post-hoc Conover test for the posdis scores.

	Temporal+L RG	Temporal RG	Temporal+L TRG	Temporal RG
Temporal+L RG	1	1	1	0.082919
Temporal RG	1	1	1	0.015836
Temporal+L TRG	1	1	1	0.045470
Temporal RG	0.082919	0.015836	0.045470	1

Table 41: p values of the post-hoc Conover test for the posdis scores.

	TemporalR+L RG	TemporalR RG	TemporalR+L TRG	TemporalR RG
TemporalR+L RG	1	1	0.149973	1
TemporalR RG	1	1	0.042950	1
TemporalR+L TRG	0.149973	0.042950	1	0.248096
TemporalR RG	1	1	0.248096	1

Table 42: p values of the post-hoc Conover test for the posdis scores.

	Attention+L RG	Attention RG	Attention+L TRG	Attention RG
Attention+L RG	1	0.394157	0.024266	0.394157
Attention RG	0.394157	1	0.001381	0.068950
Attention+L TRG	0.024266	0.001381	1	0.394157
Attention RG	0.394157	0.068950	0.394157	1

Table 43: p values of the post-hoc Conover test for the posdis scores.

F.2.6 BAG-OF-WORDS DISENTANGLEMENT POST-HOC CONOVER ANALYSIS WITHIN NETWORK TYPES

	Base+L RG	Base RG	Base+L TRG	Base RG
Base+L RG	1	1	0.001331	0.843365
Base RG	1	1	0.008259	1
Base+L TRG	0.001331	0.008259	1	0.034571
Base RG	0.843365	1	0.034571	1

Table 44: p values of the post-hoc Conover test for the bosdis scores.

	Temporal+L RG	Temporal RG	Temporal+L TRG	Temporal RG
Temporal+L RG	1	0.023856	0	0.000197
Temporal RG	0.023856	1	0	0.135339
Temporal+L TRG	0	0	1	0
Temporal RG	0.000197	0.135339	0	1

Table 45: p values of the post-hoc Conover test for the bosdis scores.

	TemporalR+L RG	TemporalR RG	TemporalR+L TRG	TemporalR RG
TemporalR+L RG	1	0.043151	0	0.878130
TemporalR RG	0.043151	1	0	0.043455
TemporalR+L TRG	0	0	1	0
TemporalR RG	0.878130	0.043455	0	1

Table 46: p values of the post-hoc Conover test for the bosdis scores.

	Attention+L RG	Attention RG	Attention+L TRG	Attention RG
Attention+L RG	1	0.748879	0.000001	0.822917
Attention RG	0.748879	1	0.000112	0.822917
Attention+L TRG	0.000001	0.000112	1	0.000003
Attention RG	0.822917	0.822917	0.000003	1

Table 47: p values of the post-hoc Conover test for the bosdis scores.

F.3 Analysis Between Network Types

F.3.1 ACCURACY POST-HOC CONOVER ANALYSIS ACROSS NETWORK TYPES

We do not list all the Kruskal-Wallis H-test p values individually, as they are all below the threshold value of 0.001.

	Base	Temporal	TemporalR	Attention
Base	1	0.000317	0.330549	0
Temporal	0.000317	1	0.006967	0
TemporalR	0.330549	0.006967	1	0
Attention	0	0	0	1

Table 48: p values of the post-hoc Conover test for the accuracy scores on the Always Same environment.

	Base	Temporal	TemporalR	Attention
Base	1	0.000005	0.235654	0
Temporal	0.000005	1	0.000513	0
TemporalR	0.235654	0.000513	1	0
Attention	0	0	0	1

Table 49: p values of the post-hoc Conover test for the accuracy scores on the Never Same environment.

	Base	Temporal	TemporalR	Attention
Base	1	0.000001	0.213130	0
Temporal	0.000001	1	0.000186	0
TemporalR	0.213130	0.000186	1	0
Attention	0	0	0	1

Table 50: p values of the post-hoc Conover test for the accuracy scores on the RG environment.

	Base	Temporal	TemporalR	Attention
Base	1	0.000184	0.909507	0
Temporal	0.000184	1	0.000195	0
TemporalR	0.909507	0.000195	1	0
Attention	0	0	0	1

Table 51: p values of the post-hoc Conover test for the accuracy scores on the RG Hard environment.

	Base	Temporal	TemporalR	Attention
Base	1	0.000011	0.337959	0
Temporal	0.000011	1	0.000422	0
TemporalR	0.337959	0.000422	1	0
Attention	0	0	0	1

Table 52: p values of the post-hoc Conover test for the accuracy scores on the TRG environment.

	Base	Temporal	TemporalR	Attention
Base	1	0.676719	0.763523	0.000035
Temporal	0.676719	1	0.724056	0.003208
TemporalR	0.763523	0.724056	1	0.000110
Attention	0.000035	0.003208	0.000110	1

Table 53: p values of the post-hoc Conover test for the accuracy scores on the TRG Hard environment.

F.3.2 COMPOSITIONALITY POST-HOC CONOVER ANALYSIS ACROSS NETWORK TYPES

We provide a full breakdown of the post-hoc Conover analysis of the compositionality scores. However, the p value of the Kruskal-Wallis H-test for the posdis metric was above the 0.001 threshold ($p = 0.10$), and so this analysis may not be statistically significant.

	Base	Temporal	TemporalR	Attention
Base	1	0	0.000020	0
Temporal	0	1	0.001046	0.002049
TemporalR	0.000020	0.001046	1	0
Attention	0	0.002049	0	1

Table 54: p values of the post-hoc Conover test for the topographic similarity scores.

	Base	Temporal	TemporalR	Attention
Base	1	0.274577	1	1
Temporal	0.274577	1	0.294687	0.136762
TemporalR	1	0.294687	1	1
Attention	1	0.136762	1	1

Table 55: p values of the post-hoc Conover test for the posdis scores.

	Base	Temporal	TemporalR	Attention
Base	1	0.003442	0.813492	0.003169
Temporal	0.003442	1	0.032353	0.941568
TemporalR	0.813492	0.032353	1	0.032353
Attention	0.003169	0.941568	0.032353	1

Table 56: p values of the post-hoc Conover test for the bosdis scores.

F.3.3 TEMPORALITY POST-HOC CONOVER ANALYSIS ACROSS NETWORK TYPES

We do not list all the Kruskal-Wallis H-test p values individually, as they are all below the threshold value of 0.001.

	Base	Temporal	TemporalR	Attention
Base	1	0	0	0
Temporal	0	1	0	0
TemporalR	0	0	1	0
Attention	0	0	0	1

Table 57: p values of the post-hoc Conover test for the $M_{\ominus 1}$ scores on the Always Same environment.

	Base	Temporal	TemporalR	Attention
Base	1	0	0	0
Temporal	0	1	0.049232	0
TemporalR	0	0.049232	1	0
Attention	0	0	0	1

Table 58: p values of the post-hoc Conover test for the $M_{\ominus 2}$ scores on the Always Same environment.

	Base	Temporal	TemporalR	Attention
Base	1	0	0.000001	0
Temporal	0	1	0	0
TemporalR	0.000001	0	1	0
Attention	0	0	0	1

Table 59: p values of the post-hoc Conover test for the $M_{\ominus 3}$ scores on the Always Same environment.

	Base	Temporal	TemporalR	Attention
Base	1	0	0	0
Temporal	0	1	0	0
TemporalR	0	0	1	0
Attention	0	0	0	1

Table 60: p values of the post-hoc Conover test for the $M_{\ominus 4}$ scores on the Always Same environment.

	Base	Temporal	TemporalR	Attention
Base	1	0	0	0
Temporal	0	1	0	0
TemporalR	0	0	1	0
Attention	0	0	0	1

Table 61: p values of the post-hoc Conover test for the $M_{\ominus 5}$ scores on the Always Same environment.

	Base	Temporal	TemporalR	Attention
Base	1	0	0	0
Temporal	0	1	0	0
TemporalR	0	0	1	0
Attention	0	0	0	1

Table 62: p values of the post-hoc Conover test for the $M_{\ominus 6}$ scores on the Always Same environment.

	Base	Temporal	TemporalR	Attention
Base	1	0	0	0
Temporal	0	1	0	0
TemporalR	0	0	1	0
Attention	0	0	0	1

Table 63: p values of the post-hoc Conover test for the $M_{\ominus 7}$ scores on the Always Same environment.

	Base	Temporal	TemporalR	Attention
Base	1	0	0	0
Temporal	0	1	0	0
TemporalR	0	0	1	0
Attention	0	0	0	1

Table 64: p values of the post-hoc Conover test for the $M_{\ominus 8}$ scores on the Always Same environment.

	Base	Temporal	TemporalR	Attention
Base	1	0	0	0
Temporal	0	1	0.031283	0.000163
TemporalR	0	0.031283	1	0.116839
Attention	0	0.000163	0.116839	1

Table 65: p values of the post-hoc Conover test for the $M_{\ominus 1}$ scores on the TRG environment.

	Base	Temporal	TemporalR	Attention
Base	1	0	0	0
Temporal	0	1	0	0
TemporalR	0	0	1	0.017773
Attention	0	0	0.017773	1

Table 66: p values of the post-hoc Conover test for the $M_{\ominus 2}$ scores on the TRG environment.

	Base	Temporal	TemporalR	Attention
Base	1	0	0	0
Temporal	0	1	0	0.005879
TemporalR	0	0	1	0
Attention	0	0.005879	0	1

Table 67: p values of the post-hoc Conover test for the $M_{\ominus 3}$ scores on the TRG environment.

	Base	Temporal	TemporalR	Attention
Base	1	0	0	0
Temporal	0	1	0	0
TemporalR	0	0	1	0
Attention	0	0	0	1

Table 68: p values of the post-hoc Conover test for the $M_{\ominus 4}$ scores on the TRG environment.

	Base	Temporal	TemporalR	Attention
Base	1	0	0	0
Temporal	0	1	0	0.094208
TemporalR	0	0	1	0
Attention	0	0.094208	0	1

 Table 69: p values of the post-hoc Conover test for the $M_{\ominus 5}$ scores on the TRG environment.

	Base	Temporal	TemporalR	Attention
Base	1	0	0	0
Temporal	0	1	0	0.535328
TemporalR	0	0	1	0
Attention	0	0.535328	0	1

 Table 70: p values of the post-hoc Conover test for the $M_{\ominus 6}$ scores on the TRG environment.

	Base	Temporal	TemporalR	Attention
Base	1	0	0	0
Temporal	0	1	0.000006	0.098090
TemporalR	0	0.000006	1	0
Attention	0	0.098090	0	1

 Table 71: p values of the post-hoc Conover test for the $M_{\ominus 7}$ scores on the TRG environment.

	Base	Temporal	TemporalR	Attention
Base	1	0	0	0
Temporal	0	1	0.000001	0.000911
TemporalR	0	0.000001	1	0
Attention	0	0.000911	0	1

 Table 72: p values of the post-hoc Conover test for the $M_{\ominus 8}$ scores on the TRG environment.

	Base	Temporal	TemporalR	Attention
Base	1	0	0	0
Temporal	0	1	0.000077	0
TemporalR	0	0.000077	1	0.032247
Attention	0	0	0.032247	1

 Table 73: p values of the post-hoc Conover test for the $M_{\ominus 1}$ scores on the TRG Hard environment.

	Base	Temporal	TemporalR	Attention
Base	1	0	0	0
Temporal	0	1	0	0
TemporalR	0	0	1	0.008141
Attention	0	0	0.008141	1

Table 74: p values of the post-hoc Conover test for the $M_{\ominus 2}$ scores on the TRG Hard environment.

	Base	Temporal	TemporalR	Attention
Base	1	0	0	0
Temporal	0	1	0	0.041111
TemporalR	0	0	1	0.000072
Attention	0	0.041111	0.000072	1

Table 75: p values of the post-hoc Conover test for the $M_{\ominus 3}$ scores on the TRG Hard environment.

	Base	Temporal	TemporalR	Attention
Base	1	0	0	0
Temporal	0	1	0	0
TemporalR	0	0	1	0
Attention	0	0	0	1

Table 76: p values of the post-hoc Conover test for the $M_{\ominus 4}$ scores on the TRG Hard environment.

	Base	Temporal	TemporalR	Attention
Base	1	0	0	0
Temporal	0	1	0	0.893338
TemporalR	0	0	1	0
Attention	0	0.893338	0	1

Table 77: p values of the post-hoc Conover test for the $M_{\ominus 5}$ scores on the TRG Hard environment.

	Base	Temporal	TemporalR	Attention
Base	1	0	0	0
Temporal	0	1	0	0.216498
TemporalR	0	0	1	0
Attention	0	0.216498	0	1

Table 78: p values of the post-hoc Conover test for the $M_{\ominus 6}$ scores on the TRG Hard environment.

	Base	Temporal	TemporalR	Attention
Base	1	0	0	0
Temporal	0	1	0.000041	0.335553
TemporalR	0	0.000041	1	0.000005
Attention	0	0.335553	0.000005	1

Table 79: p values of the post-hoc Conover test for the $M_{\ominus 7}$ scores on the TRG Hard environment.

	Base	Temporal	TemporalR	Attention
Base	1	0	0	0
Temporal	0	1	0.000119	0.075538
TemporalR	0	0.000119	1	0
Attention	0	0.075538	0	1

Table 80: p values of the post-hoc Conover test for the $M_{\ominus 8}$ scores on the TRG Hard environment.